the plant journal

The Plant Journal (2025) 121, e70059 doi: 10.1111/tpj.70059

EIL (ethylene-insensitive 3-like) transcription factors in apple affect both ethylene- and cold response-dependent fruit ripening

Jiao Feng[1,2], Mindy Y. Wang[1], Xiuyin Chen[1], Sumathi Tomes[1], Jianmin Tao[2], Ross G. Atkinson[1] and Niels J. Nieuwenhuizen[1,*]

[1]The New Zealand Institute for Plant and Food Research Limited (PFR), Mount Albert Research Centre, Private Bag 92169, Auckland 1142, New Zealand, and

[2]College of Horticulture, Nanjing Agricultural University, Nanjing 210095, China

Received 12 December 2024; revised 29 January 2025; accepted 10 February 2025.
*For correspondence (e-mail niels.nieuwenhuizen@plantandfood.co.nz).

SUMMARY

EIN3/EIL (ethylene-insensitive 3/EIN3-like) transcription factors are positive downstream transcriptional regulators of ethylene signalling. In apple (*Malus* × *domestica*), a small family of MdEIL genes was identified, with four expressed in fruit. Transgenic lines were generated to manipulate *MdEIL1* expression, and fruits were sampled at harvest maturity and after cold treatment. Their fruit ripening behaviour was compared with control lines and contrasted to a *ACC OXIDASE 1* antisense line (ACO1as) which produced no ripening associated ethylene. Two transgenic lines showed strong co-suppression of *MdEIL1–4* expression as well as reduced ethylene production, softening and aroma production, while one overexpressing line showed enhanced ripening. Key genes involved in ethylene biosynthesis and ethylene-dependent genes involved in cell wall modification (*MdXTH1*, *MdβGAL*) and aroma biosynthesis (*MdAFS1*, *MdoOMT1*) were downregulated in the co-suppressed lines. Co-suppressed lines showed reduced softening/volatile production after cold treatment and in contrast to the ACO1as line, expression of cold response-dependent genes (*MdCBF2*, dehydrins *MdDHN2, −14, −16* and *MdNAC29a*) remained cold-repressed. The action of MdEILs was shown using dual-luciferase reporter assays to occur through direct activation of *MdAFS1*, *MdXTH1* and *MdβGAL* promoters. Exogenous ethylene was unable to further stimulate ripening promoter activation, but cold treatment could. Promoter deletion analysis identified potential EIL binding sites in the *MdAFS1* and *MdβGAL* promoters and electrophoretic mobility shift assays showed that MdEIL1–3 could all bind to a 32 bp fragment in the *MdAFS1* promoter. Together these results indicate that MdEILs contribute to a suite of apple fruit ripening attributes via activation of genes in an ethylene-dependent manner, but also in response to cold.

Keywords: aroma production, cold treatment, ethylene signalling, *Malus domestica*, promoter activation, softening.

INTRODUCTION

Fruit ripening is often accompanied by changes in colour, sugar/acid content, flavour, aroma and texture (Deng et al., 2022; Li et al., 2016; Wang et al., 2020). These changes allow for the fruit to be presented in the most attractive ways to fruit-dispersing frugivores and omnivores, and have also been selected and bred during domestication to appeal to human consumers (Bai & Lindhout, 2007; Khan et al., 2014; Rao et al., 2021). The complex changes in fruit physiology are driven by a directed programme of molecular and biochemical changes that is influenced by genetic backgrounds, environmental factors and phytohormones (Fu et al., 2021; Ji & Wang, 2021). Fleshy fruit have traditionally been divided into non-climacteric (NC) and climacteric (CL) ripening groups based on differences in their ripening physiology behaviour (Kou et al., 2021). For example, strawberry, grape and citrus need to be harvested when ripening programmes have been completed, and these NC fruits do not show a respiratory climacteric or produce a large burst of ethylene after harvest (Liu et al., 2024). In contrast, CL species such as pear, tomato and kiwifruit can be harvested before ripening is complete and show characteristic bursts in respiration and associated ethylene production after harvest, during the final ripening stages (Giovannoni et al., 2017; Li et al., 2021; Payasi

& Sanwal, 2010). Whilst there appear to be clear distinctions between both modes of ripening, many fruit show examples of both modes, for example in melon, where both NC and CL varieties exist (Los et al., 2024). It is now well established that CL fruits share a common mechanism of ripening regulation, that is, via ethylene regulation (Alexander & Grierson, 2002; Fenn & Giovannoni, 2021). These fruit not only show a burst of ethylene production at the onset of fruit ripening, but also respond to the application of exogenous ethylene by triggering CL fruit ripening, and conversely, inhibiting ethylene action can effectively arrest CL fruit ripening (Zhang et al., 2017a). This mode of ethylene regulation has been commercially exploited to control and improve the shelf-life of many CL fruits (Ebrahimi et al., 2022; Martínez-Romero et al., 2007).

Ethylene biosynthesis involves the conversion of *S*-adenosyl methionine (SAM) to 1-aminocyclopropane-1-carboxylic acid (ACC) by the enzyme ACC synthase (ACS), followed by the formation of ethylene by ACC oxidase (ACO) (An et al., 2018b; Barry et al., 2000; Hu et al., 2019). As the direct precursor of ethylene, ACC formation is generally considered to be the rate-limiting step (Li et al., 2016; Lin et al., 2009), but ethylene formation is also influenced by ACO levels. Two systems of ethylene regulation have been well established in higher plants: system 1 is ethylene-autoinhibitory and responsible for basal ethylene production in non-ripening and non-climacteric fruits and is involved in wound ethylene production, whilst system 2 is responsible for producing autocatalytic ethylene in climacteric fruit ripening (Barry et al., 2000; Huang et al., 2022; Ji & Wang, 2021; Li et al., 2016; Nieuwenhuizen et al., 2015; Yue et al., 2020). Autocatalytic regulation points to a positive feedback loop controlling ethylene synthesis (Dolgikh et al., 2019). The linear ethylene signalling pathway starts with the perception of ethylene by a family of receptors embedded in the membranes of the endoplasmic reticulum (ER). Subsequently, downstream signalling is controlled through several components, including Raf-like serine/threonine kinase constitutive triple response 1 (CTR1) and ethylene-insensitive 2 (EIN2). The transcription factor (TF) family EIN3/EIL (ethylene-insensitive 3/EIN3-like) are primary positive regulators of ethylene responses, inducing secondary and tertiary TFs such as ethylene-response factors (ERFs) and MYBs, which relay the signal and enhance/repress the expression of further downstream ethylene-responsive genes (An et al., 2018b; Dolgikh et al., 2019; Hu et al., 2019; Huang et al., 2022; Ji & Wang, 2021; Li et al., 2016; Qiu et al., 2015). EIN3/EIL TFs function through binding to the primary ethylene-response element (PERE) or EIL conserved binding sequence motifs (ECBS) of gene promoters (Chen et al., 2004; Dolgikh et al., 2019; Ji & Wang, 2021; Tieman et al., 2001). In Arabidopsis, knockouts of both *AtEIN3* and *AtEIL1* combined resulted in a complete ethylene-insensitive phenotype (Alonso et al., 2003). In tomato, antisense lines with the greatest reduction in total EIL expression exhibited the greatest ethylene insensitivity (Tieman et al., 2001). A series of loss-of-function tomato mutants in the *SlEIL1–4* genes were analysed and showed significant functional redundancy, and demonstrated that ethylene plays a positive role in tomato fruit growth and ripening (Huang et al., 2022). EIN3 protein levels are controlled by 26S proteasomal degradation through interaction with EIN3-binding F-box (EBF) proteins in the absence of ethylene (Gagne et al., 2004).

Cold is an important abiotic stress characterised by below optimal temperature exposure and can be divided into chilling stress (above freezing temperature, >0°C) and freezing stress (<0°C). Cold stress affects plant survival as well fruit development and ripening (An et al., 2021; Xie et al., 2018), but conversely cold is also used to prolong the storage of fruit by inhibiting respiration and other ripening processes. Alterations in physiology and gene expression patterns in response to cold have been extensively studied (Juurakko et al., 2021), and some of the molecular mechanisms underpinning the response to cold have been elucidated. Cold sensing in part occurs by increased membrane rigidity and by the activation of mechanosensitive Ca^{2+} channels (Ding & Pickard, 1993), for example COLD1 in rice is a protein involved in the cold signalling by interacting with a G protein to activate the Ca^{2+} channel for temperature sensing (Ma et al., 2015). C-repeat binding factor (CBF) TFs have been shown to play roles in the downstream plant response to cold stress (Barrero-Gil & Salinas, 2017) and redox-mediated structural and functional switching of the CBFs appears to be a pivotal feature in plant cold tolerance responses (Wi et al., 2022). CBF expression is induced by another TF called ICE1 (Inducer of CBF Expression 1) (Chinnusamy et al., 2003). In tomato, *SlCBF1* appears to be important for cold tolerance in vegetative tissues, but not in fruit (Weiss & Egea-Cortines, 2009), while in kiwifruit, *CBF2* and *CBF3* were induced by cold (0–10°C) in fruit (Gunaseelan et al., 2019). CBFs are master TFs that are rapidly induced by cold and bind to the C-repeat/dehydration-responsive motif (CRT/DRE) in the promoter region of the downstream cold-responsive (COR) genes, such as dehydrins involved in a number of protective processes in the cell (Peng et al., 2014; Vazquez-Hernandez et al., 2017) and AtCOR15a involved in protecting chloroplast membranes during freezing (Wang & Hua, 2009). AtEIN3 negatively regulates the expression of CBFs in Arabidopsis (Shi et al., 2012), suggesting a complex interplay between ethylene and cold response pathways.

Apple (*Malus* × *domestica* Borkh.) is a classic climacteric fruit and ethylene production influences many key ripening traits including softening, flavour and aroma production. Downregulation of the ripening-related ethylene biosynthesis gene *ACC OXIDASE 1* (*MdACO1*) by

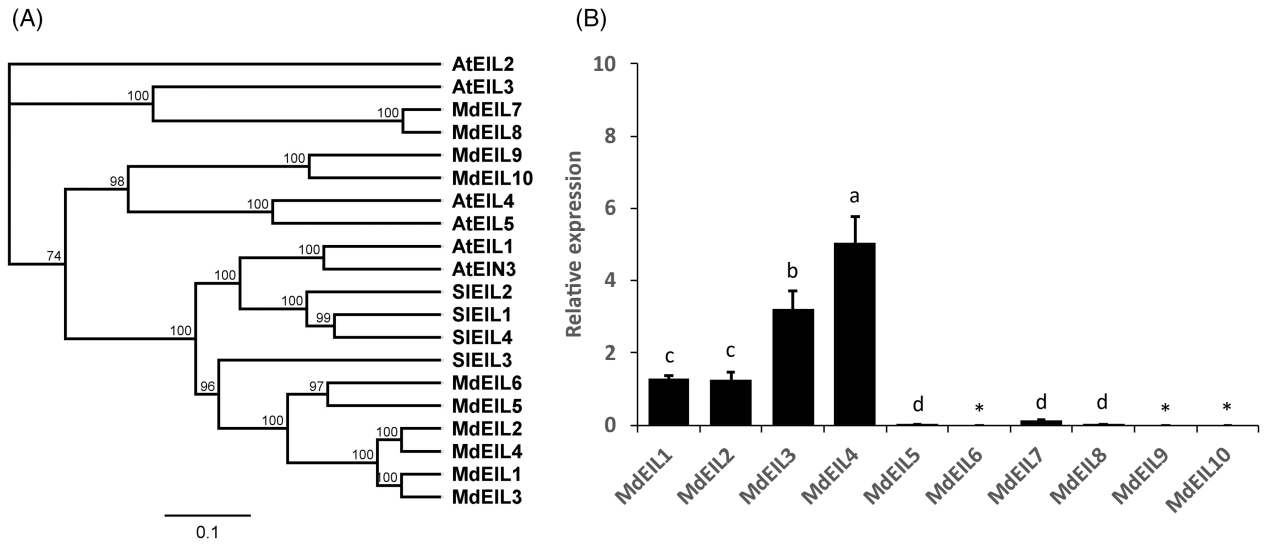

Figure 1. Phylogenetics of the MdEIL family in apple and expression of *MdEIL1–10* in apple fruit at harvest.
(A) Phylogenetic tree of EIL transcription factors of Arabidopsis (At), *Solanum lycopersicum* L. (tomato, Sl) and apple (Md) constructed in Geneious Prime.
(B) Relative quantification gene expression was determined by RT-qPCR using gene-specific primers (Table S2). Data are presented as mean ± SE ($n = 6$) and normalised against four reference genes. Lower case letters indicate significant differences at the level of $P < 0.05$ among different genes based on one-way ANOVA followed by Duncan's test.
**MdEIL6, MdEIL9* and *MdEIL10* expression were not detected.

antisense results in inhibition of ethylene production, which delays ripening and fruit softening, as well as reducing sugar accumulation and aroma release (Johnston et al., 2009; Schaffer et al., 2007). Ethylene induces the expression of cell wall-modifying enzymes implicated in softening, such as endo-polygalacturonase1 (*MdPG1*), β-galactosidase (*MdβGAL*) and xyloglucan endo-transglucosylase/hydrolase (*MdXTH1*) (Atkinson et al., 2012; Yang et al., 2018; Zhang, Wang, et al., 2017) and genes involved in volatile aroma production, such as α-farnesene synthase (*MdAFS1*) (Pechous & Whitaker, 2004) for the production of the sesquiterpene α-farnesene (Souleyre et al., 2019), and O-methyltransferase *MdoOMT1* involved in estragole biosynthesis (Yauk et al., 2015). MdEIL1 has been shown to directly bind to the *MdMYB1* promoter to induce anthocyanin accumulation and fruit colouration (An et al., 2018b), and to activate the *MdPG1* promotor to promote softening (Tacken et al., 2010).

Regulation of the cold response in apple is less well described. NAC TFs have been shown to be involved, with *MdNAC029* repressing *MdCBF1, 4* expression in apple calli (An, Li, et al., 2018), while *MdNAC104* positively regulated cold tolerance via CBF-dependent and CBF-independent pathways (Mei et al., 2023). The *MdPG1* promoter was transactivated by *MdCBF2* in apple cell-suspensions, and transactivation of *MdPG1* was further enhanced by exogenous ethylene in tobacco leaves (Tacken et al., 2010). Using *ACC OXIDASE1* suppressed apple lines, it was established that *MdPG1* participates in initiating fruit softening by cold temperature in 'Royal Gala' apple, independently from ethylene (Tacken et al., 2010). Overexpression of a peach CBF gene (*PpCBF1*) in apple promoted cold hardiness, dormancy and leaf pigmentation, and inhibited plant growth (Artlip et al., 2014), while dehydrin induction was associated with cold acclimatisation during dormancy (Falavigna et al., 2015).

In this study, *MdEIL1* overexpression lines and lines silenced/co-suppressed for *MdEIL1–4* (MdEILko) were identified and characterised. The *MdEIL1–4* silenced lines showed strong reductions in ethylene production, softening and aroma production compared with wild-type controls. However, in contrast to fruit from *ACC OXIDASE1* antisense (ACO1as) and wild-type lines, the MdEILko fruit showed reduced softening after cold treatment and induction of cold-related genes. Our results reveal the importance of MdEIL TFs in fruit ripening in apple and shed new light on the regulatory mechanism of climacteric fruit ripening and the interplay between ethylene and cold.

RESULTS

Ten MdEIL gene family members (designated *MdEIL1–10*) were identified in the apple genome (Table S1) by BLASTP searching with the *Arabidopsis thaliana* EIN3 TF (Guo & Ecker, 2004). Three of these genes were previously published as *MdEIL1–3* by Tacken et al. (2010). *MdEIl1–4* showed >82% overall nucleotide sequence identity, while *MdEIL5* and *MdEIL6* shared 85% DNA sequence identity and >72% with *MdEIL1–4* (Figure S1a). *MdEIL7–10* showed lower sequence identity with *MdEIL1–6* (between 31% and

45% identity) with highest identity located at the N-terminus (Figure S1b).

Alignment of the deduced amino acid sequences of MdEIL1–10 (Figure S1c) demonstrated that they grouped into five pairs of two genes (Figure 1A). Four pairs (MdEIL1/2, MdEIL2/4, MdEIL5/6, MdEIL7/8) may potentially represent homeologs that have arisen due to the ancient duplication of the apple genome (Velasco et al., 2010) as these pairs were located on corresponding homoeologous chromosomes (Table S1). MdEIL2 and MdEIL5 appear to be ancient tandem paralogs, as they only sit 17 kb apart on chromosome 7, while the corresponding respective homeologs MdEIL4 and MdEIL7 are located in tandem 17 kb apart on chromosome 2. Phylogenetic analysis indicated that MdEIL1–6 clustered most closely to AtEIN3 and AtEIL1 from *A. thaliana*, as well as SlEIL1–4 from *Solanum lycopersicum* (Figure 1A; Figure S1c). MdEIL7, 8 were most similar to AtEIL3, while MdEIL9, 10 were most similar to AtEIL4 and 5 (Weiss & Egea-Cortines, 2009). *AtEIL3* (SLIM1) has been reported to play a central role in sulphur response and metabolism (Maruyama-Nakashita et al., 2006), while *AtEIL4* was found to exhibit restricted expression in the Arabidopsis embryo (Jeong et al., 2014).

Expression of *MdEIL1–10* was assessed in tissues from apple fruit at harvest maturity relative to the geometrical mean of four reference genes. *MdEIL1–4* showed high expression in fruits while expression of *MdEIL5–10* was much lower in fruit at harvest (Figure 1B).

Molecular characterisation of MdEIL1 transgenic lines

To characterise the function of the MdEILs in apple, an overexpression construct pHEX2-35S:EIL1 was stably transformed into 'Royal Gala' apple plants. In 2016, 10 35S:EIL1 transgenic lines were regenerated as well as four 35S:GFP control lines and confirmed by PCR to contain the expected transgene (Figure S2). Eight independent transgenic lines subsequently yielded enough fruit over two seasons (2023 and 2024 harvests) for further analysis, including six 35S:EIL1 and two 35S:GFP control lines. The transgenic lines were grown alongside further wild-type 'Royal Gala' plants (WT2, WT5 and WT7) and two clonal *MdACO1*-antisense (ACO1as) lines (Schaffer et al., 2007). No apparent visible vegetative phenotypes were observed in the transgenic lines and flowers and fruit developed normally.

The expression of *MdEIL1* was assessed by RT-qPCR in fruit tissue at harvest and after 10 weeks of cold treatment from the 35S:EIL1 transgenic lines, ACO1as, as well as 35S:GFP and WT controls (Figure 2A). At harvest, expression of *MdEIL1* (the sum of endogenous and transgene *MdEIL1* mRNA) was significantly higher in 35S:EIL1 lines E308, E317 and E322 compared with the controls, while expression levels in two 35S-EIL1 lines E310 and E316, and ACO1as, were low, comparable to the controls. Similar results were obtained in samples from fruit after 10 weeks of cold treatment, but lines E310 and E316 showed significantly lower levels of *MdEIL1* expression than the controls, while higher expression was detected for E317, E318 and E322 (Figure 2A).

To assess if expression of any of the other *EIL* family genes was affected by overexpression of *MdEIL1*, the expression of each gene was measured at harvest and after cold treatment (Figure 2B–D). At harvest, expression of *EIL2*, *EIL3* and *EIL4* was significantly downregulated in lines E310 and E316, compared with all control lines. After 10 weeks of cold treatment, this pattern was sustained, but line E308 also showed lower expression for *MdEIL2–4*. For line E317, *MdEIL2* expression was significantly lower, but *MdEIL3*, *4* showed no change in expression. There were no significant differences among the transgenic lines and control lines for *MdEIL5* expression levels, which was low at harvest and after 10 weeks of cold treatment (Figure S3), while expression of *MdEIL6* was not detected at either sampling time. The ACO1as line showed control levels of expression of all *EIL* genes, both at harvest and after 10 weeks of cold treatment (Figure 2; Figure S3). Together, these results indicate that 35S:EIL1 lines E310 and E316 are co-suppressed for *MdEIL1* and also co-suppressed for *MdEIL2–4*. These two lines are hereafter designated E310ko and E316ko. E317 and E322 are overexpression lines for *MdEIL1* both at harvest and after cold treatment, and are subsequently designated E317ox and E322ox. *MdEIL1–4* share over 95% nucleotide sequence identity across the 5′-end of the open reading frame (1 kb from the ATG – see Figure S1b), which explains why multiple genes can be co-suppressed simultaneously.

Ripening phenotypes of MdEIL1 transgenic lines

Ripening phenotypes of MdEIL1 transgenic lines were assessed over two harvests (Season 1 and Season 2). The physical appearance of the apple fruits from the MdEIL1 transgenic lines and controls are shown in Figure S4. Co-suppressed lines E310ko and E316ko both showed a green skin phenotype, similar to the ACO1as line, in contrast to the red blush with yellow background for the transgenic overexpression lines and controls. The appearance of the fruit did not change after cold storage.

Levels of ethylene were measured at harvest in the fruit of transgenic and control lines in Season 1 (Figure 3A) and results were similar in Season 2 (Figure S5). E317ox fruit showed significantly higher levels of ethylene production compared to the controls, while co-suppressed lines E310ko, E316ko and ACO1as all showed very low levels of ethylene production (Figure 3A). After 10 weeks of cold treatment, ethylene production was lower in all lines compared to that at harvest. Both overexpression lines E317ox and E322ox showed significantly higher ethylene production compared with the control levels, while lines E310ko, E316ko and ACO1as showed very low levels of ethylene production (Figure S5).

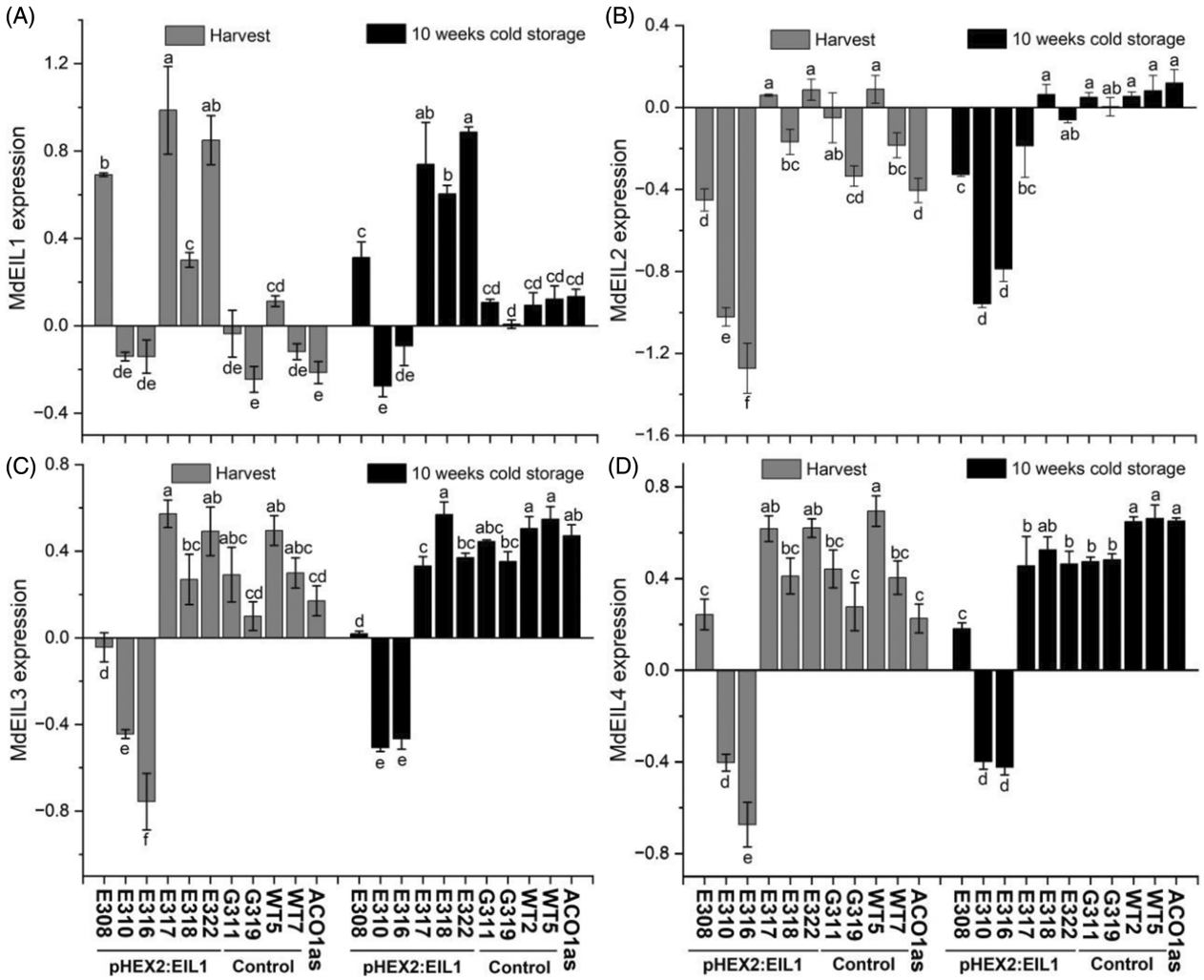

Figure 2. Expression of MdEIL1–4 in fruit of transgenic and control lines at harvest and after 10 weeks of cold treatment. Gene expression was determined by RT-qPCR using gene-specific primes (Table S2).
(A) *MdEIL1*, (B) *MdEIL2*, (C) *MdEIL3*, (D) *MdEIL4*. 35S:EIL1 lines E308, E310, E316, E317, E318, E322; control lines 35S:eGFP G311, G319; wild-type WT2, WT5, WT7; and ACO1as (ACC oxidase 1 antisense). The $\log_{10}$ of relative expression values were used for graphing and analysis, based on normalisation against four reference genes. Data are presented as mean ± SE ($n = 6$). Lowercase letters indicate significant differences at the level of $P < 0.05$ among different lines at each stage based on one-way ANOVA followed by Duncan's test.

At harvest, fruit firmness for E317ox was softer compared to the controls (Figure 3B; Figure S5), while all other lines showed similar firmness compared to the controls. After 10 weeks of cold treatment, E317ox fruit were still significantly softer, while E310ko and E316ko were firmer compared to the controls. In Season 1, ACO1as fruit showed no significant difference in firmness, either at harvest or after 10 weeks cold treatment, compared to the controls (Figure 3B). In Season 2, results were similar, apart from ACO1as fruit being firmer than the controls both at harvest and after cold treatment. In both Season 1 and 2 the ACO1as fruit were significantly softer than E310ko and E316ko after cold treatment (Figure S5).

Soluble solids content (SSC; °Brix) showed no consistent differences across either season. For example, line E317ox and ACO1as showed lower SSC in Season 1 at both harvest and after cold treatment, but this was not observed in Season 2, when line E310ko and E316ko had a lower °Brix at harvest compared to the controls in Season 1. This was not observed in Season 2 (Figure 3C; Figure S5). In both seasons, line E310ko, E316ko and ACO1as were significantly greener, which was reflected in a higher hue angle; h° (Figure 3D; Figure S5). The starch pattern index values for E310ko and E316ko were lower in both seasons at harvest, which indicated that these fruits contained more starch (Figure S5).

Aroma volatile compounds produced by MdEIL1 transgenic lines

For Season 1, headspace volatile aroma compounds produced by MdEIL1 transgenic lines and control lines at harvest

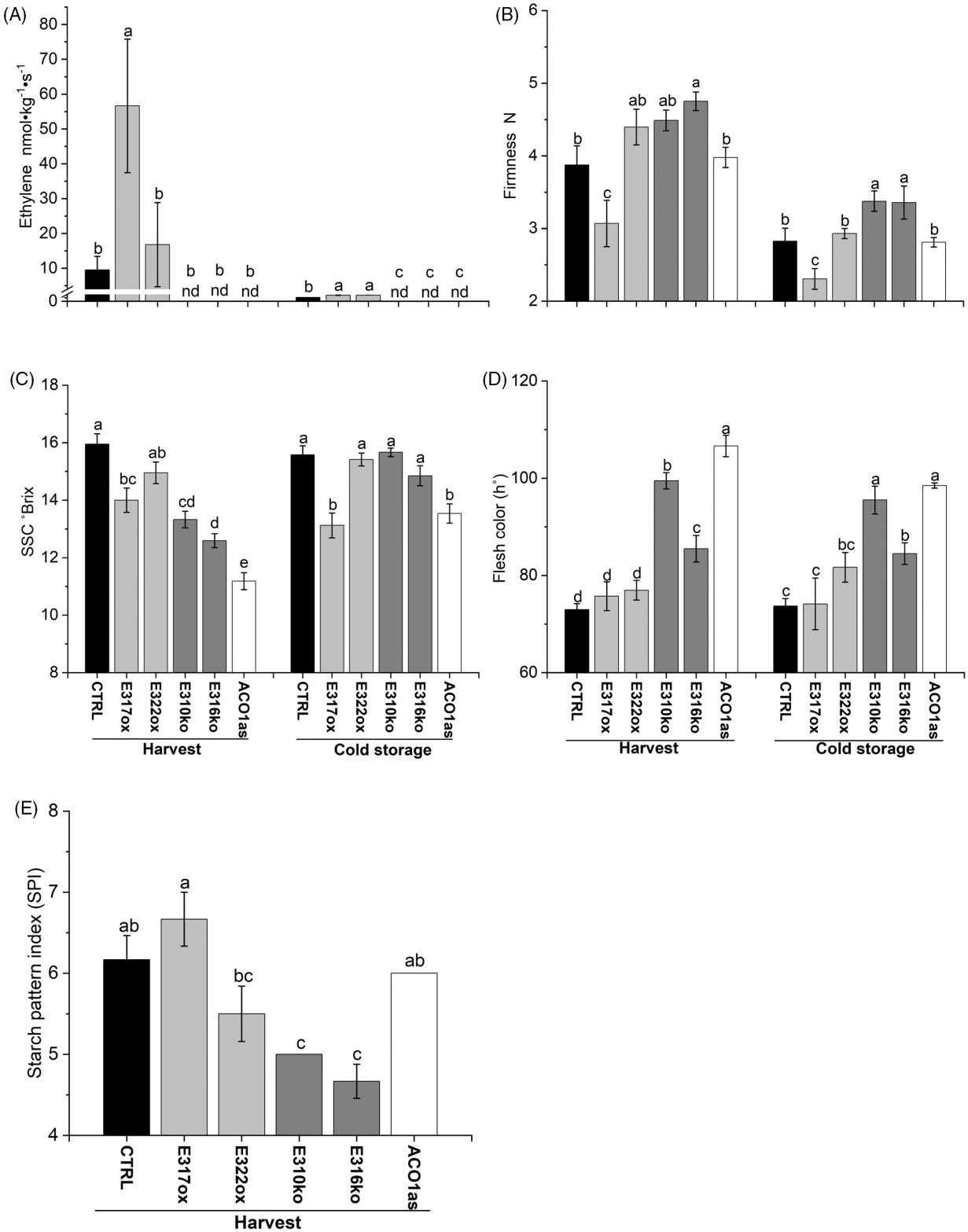

Figure 3. Ethylene production, firmness and soluble solids content of fruit from transgenic and control lines at harvest and after cold treatment for Season 1. Ethylene concentration (A), firmness (B), soluble solids content (SSC) (C), flesh colour (hue angle, h°) (D) and starch pattern index (SPI) (E). 35S:EIL1 lines = E310ko, E316ko, E317ox, E322ox; CTRL (control)= G311, G319, WT2, WT5, WT7; and ACO1as (ACC oxidase1 antisense). Nd: not detected, ethylene <0.5 nmol•kg^{-1}•s^{-1}. Data are presented as mean ± SE (n = 6). Lowercase letters indicate significant differences at the level of $P < 0.05$ among different lines at each stage using one-way ANOVA followed by Duncan's test.

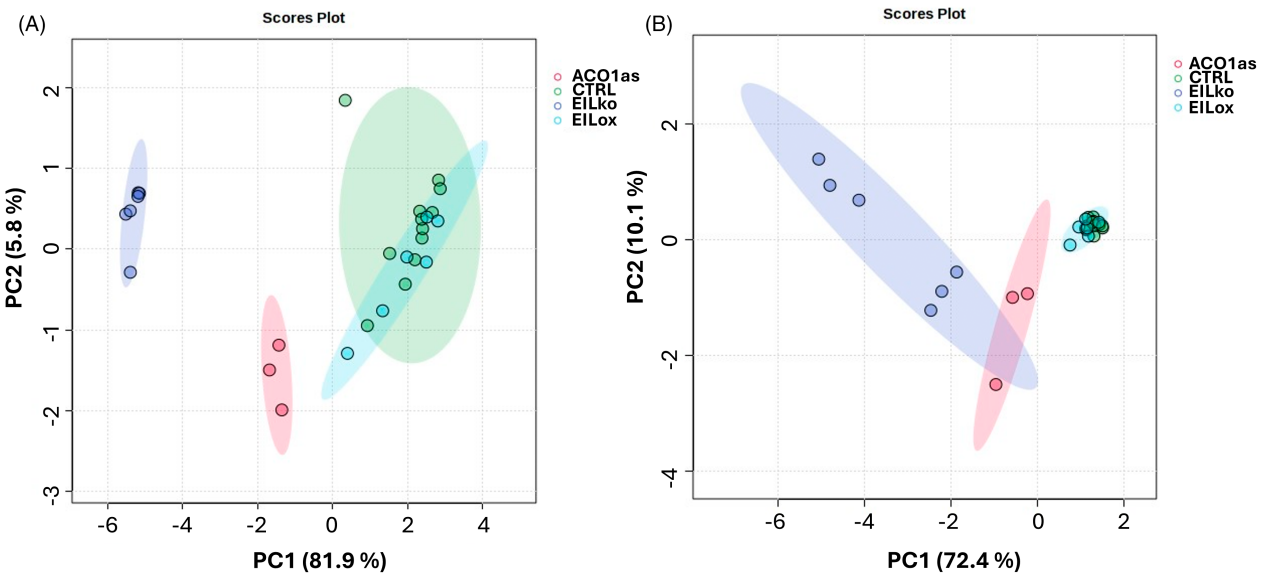

Figure 4. Principal component analysis of headspace volatiles produced by transgenic and control lines at harvest (A) and after 10 weeks cold treatment (B). Groups: ACO1as; EILko = E310ko, E316ko; EILox = E317ox, E322ox; CTRL = G311, G319, WT2, WT5, WT7. Original data were normalised by $\log_{10}$ transformation and mean centring. The 95% of confidence intervals are circled.

and after cold treatment were collected by SPME and analysed by gas chromatography-mass spectrometry (GC–MS) (Table S3). Principal component analysis of the GC–MS data was carried out with MetaboAnalyst 6.0 (https://www.metaboanalyst.ca) to understand the global differences in volatiles produced. Based on the phenotypic analysis, lines were assigned to four groups in Figure 4: MdEIL-co-suppressed lines (EILko, purple), ACO1as (red), MdEIL-overexpression lines (EILox, blue) and control lines (CTRL, green).

At harvest, 87.7% of the variability in headspace volatiles could be explained by the first two principal components, with PC1 contributing 81.9% of the total variation. An overlap was found between the EILox and control groups, while the EILko and ACO1as groups formed separate clusters (Figure 4A). The volatiles α-farnesene and (*Z*)-3-hexen-1-ol contributed strongly to the discrimination between control, EILox groups versus the EILko, ACO1as groups (Figure S6a,b). After cold treatment, 82.5% of the variability in headspace volatiles could be explained by the first two principal components, with PC1 contributing 72.4% of the total variation. Different from the samples at harvest, the scores plot showed some overlap between the EILko and ACO1as groups, with the EILox and control groups again overlapping (Figure 4B). The corresponding loading plot and biplots again indicated that higher concentrations of ripening-related volatiles such as butyl butanoate, estragole, α-farnesene and n-propyl acetate were observed in the EILox and control groups compared to E310ko and E316ko (Figure S6c,d).

Figure 5 shows the production of key aroma volatiles in more detail. At harvest, much lower levels of α-farnesene and estragole were observed in the *MdEIL*-co-suppressed lines E310ko, E316ko as well as ACO1as (Figure 5A,B). The production of the fruity aroma esters such as butyl butanoate and n-propyl acetate was also lower in *MdEIL*-co-suppressed lines E310ko, E316ko and ACO1as line compared to the controls and other transgenic lines (Figure 5C,D). In contrast, the concentration of 2-methylbutyl acetate (2MBA) was not significantly altered in the *MdEIL*-co-suppressed or ACO1as lines (Figure 5E). (*Z*)-3-hexen-1-ol concentrations were much higher in the *MdEIL1* co-suppressed lines E310ko, E316ko and ACO1as, compared with the controls (Figure 5F). This may reflect increased substrate accumulation of C6-alcohols that usually get converted by alcohol acyl-CoA transferases (AATs) into corresponding fruity esters in ripening fruit (Souleyre et al., 2014).

After cold treatment, ACO1as showed significantly higher levels of a number of volatiles compared with E310ox and E316ox, including α-farnesene, n-propyl acetate and 2MBA, but still at lower levels compared with the controls. This result further highlights that there are significant contrasts in volatile induction upon the cold response in the ethylene biosynthesis mutant (ACO1as) versus both EIL co-suppressed lines.

Expression of key ripening-related genes in MdEIL transgenic lines

The expression patterns of key genes involved in ethylene biosynthesis (*MdACO1*), cell wall modification (*MdXTH1*, *MdβGAL*) and aroma biosynthesis (*MdAFS1* and *MdoOMT1*) were investigated by RT-qPCR in the MdEIL

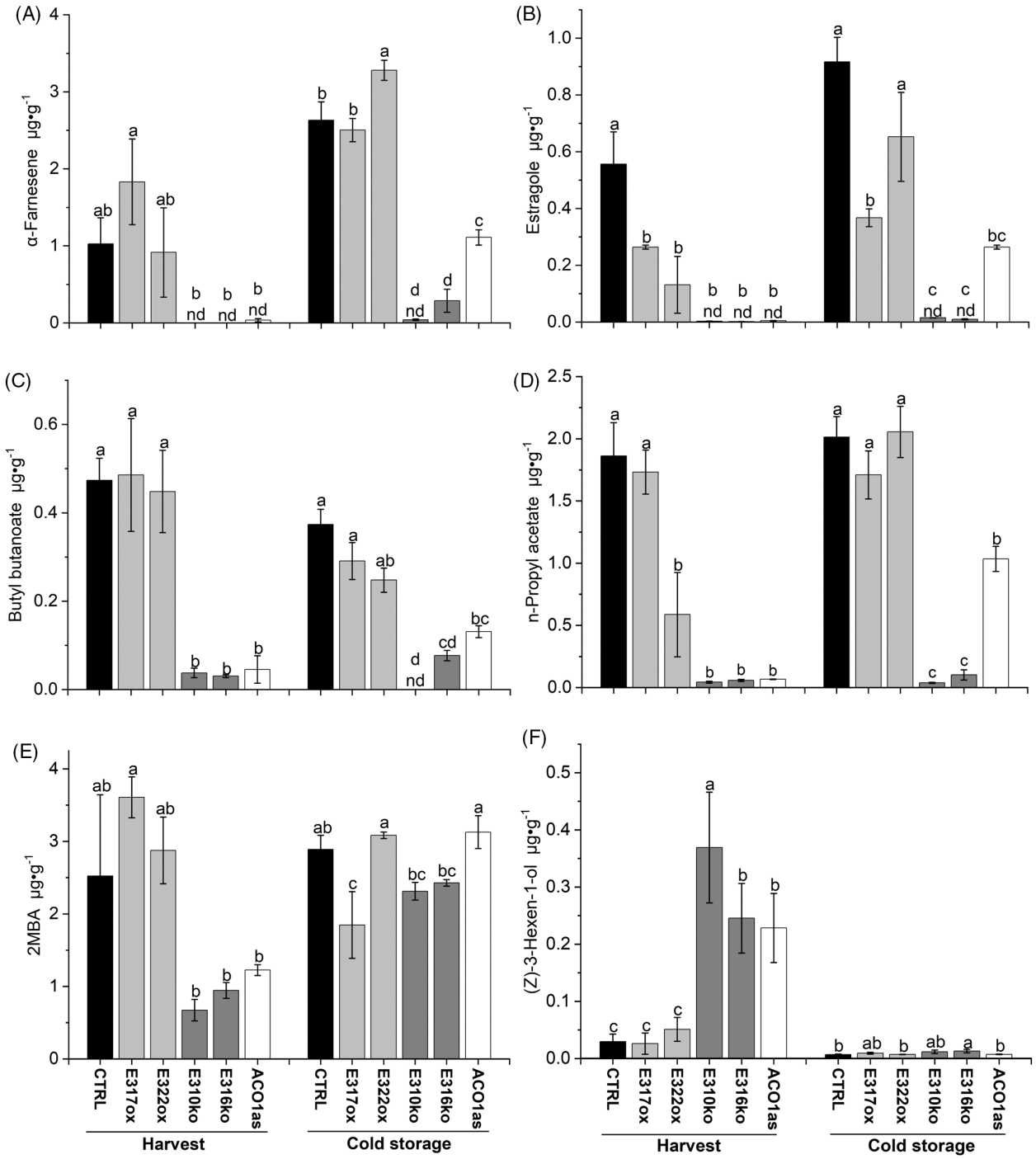

Figure 5. Concentrations in $\mu g \cdot g^{-1}$ FW of selected headspace volatiles produced by transgenic and control fruit at harvest and after 10 weeks of cold treatment (A) α-farnesene, (B) estragole, (C) butyl butanoate, (D) n-propyl acetate, (E) 2-methylbutyl acetate (2MBA), (F) (Z)-3-hexen-1-ol.
35S:EIL1 lines = E310ko, E316ko, E317ox, E322ox; CTRL (control) lines = G311, G319; wild-type = WT2, WT5, WT7; and ACO1as. Nd: not detected, concentrations <0.05 $\mu g \cdot g^{-1}$. Data (Table S3) are presented as mean ± SE (n = 6). Lowercase letters indicate significant differences at the level of $P < 0.05$ among different lines at each stage based on one-way ANOVA followed by Duncan's test.

transgenic lines and controls at harvest and after 10 weeks of cold treatment. The expression pattern of *MdACO1* was similar at both sample points and corresponded with the ethylene production results (Figure 3A). Very low levels of *MdACO1* expression were detected in transgenic lines E310ko, E316ko and ACO1as at both sample points. Overall, *MdACO1* expression was weakly upregulated after cold treatment compared to harvest in all lines (Figure 6A).

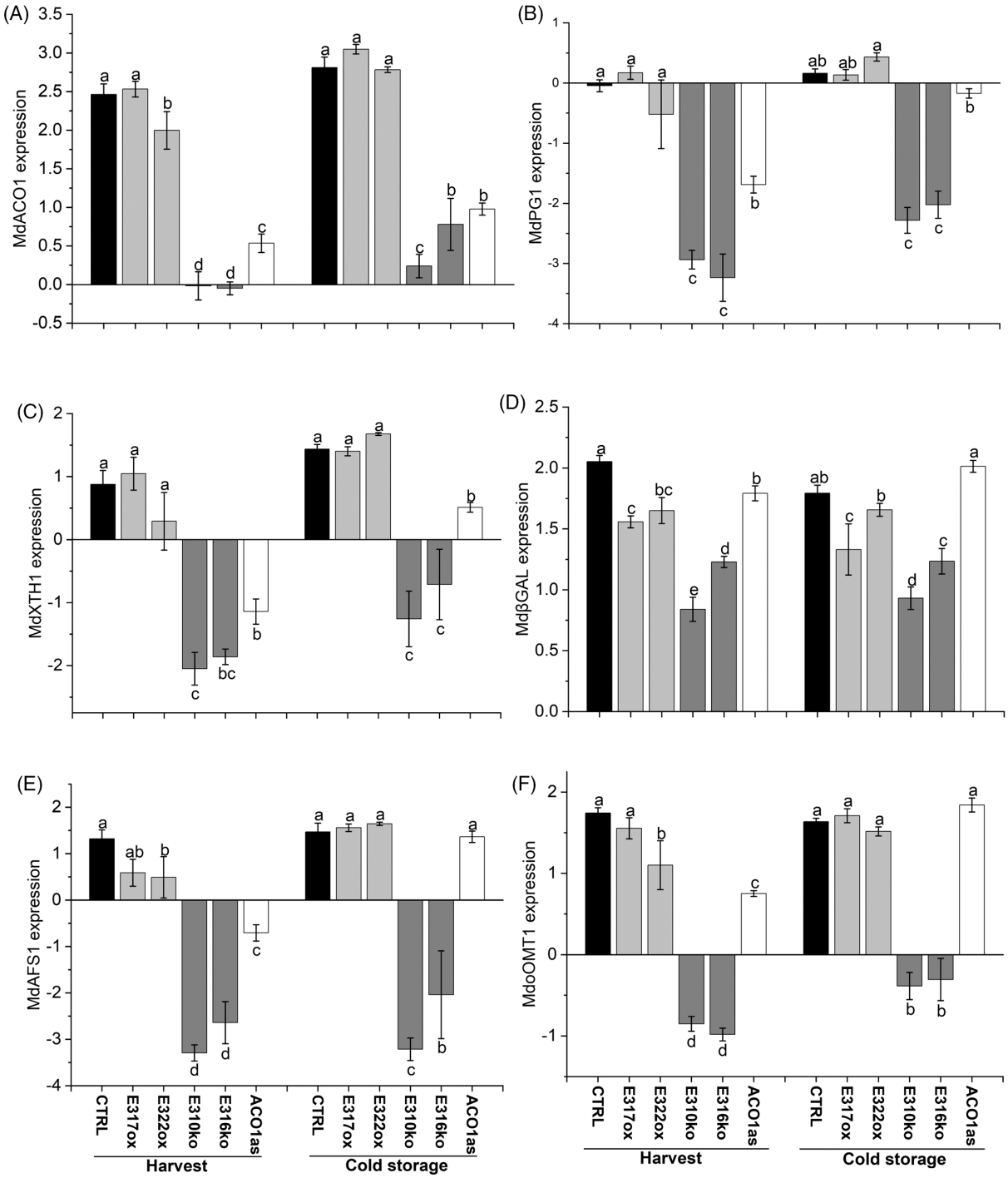

Figure 6. Expression of ethylene biosynthetic, cell wall modification and volatile aroma biosynthesis related genes in transgenic and control fruit at harvest and after cold treatment.

(A–F) Gene expression was determined by RT-qPCR using gene-specific primers (Table S2). (A) ethylene biosynthetic gene *MdACO1;* cell wall modification related genes (B) *MdPG1*, (C) *MdXTH1*, (D) *Md*β*GAL*, and volatile aroma biosynthesis related genes (E) *MdAFS1*, (F) *MdoOMT1*. 35S:EIL1 lines = E310ko, E316ko, E317ox, E322ox; CTRL (control) lines = G311, G319; wild-type = WT2, WT5, WT7; and ACO1as. Log_{10} relative expression values were used for graphing and analysis, based on normalisation against four reference genes. Data are presented as mean ± SE (n = 6). Lowercase letters indicate significant differences at the level of $P < 0.05$ among different lines at each stage based on one-way ANOVA followed by Duncan's test.

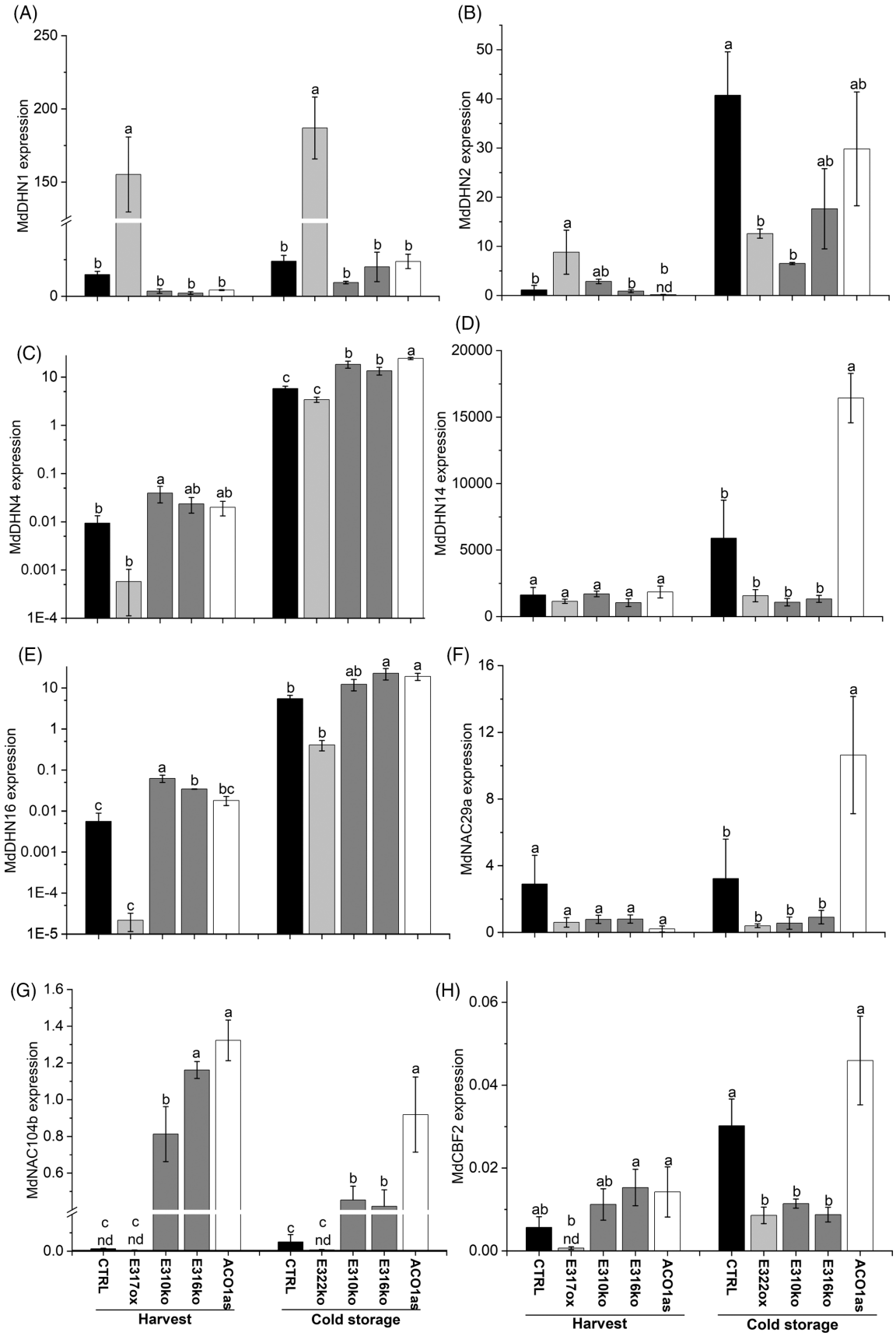

Figure 7. Expression of dehydrins (DHN), NAC and CBF transcription factors in transgenic and control fruit at harvest and after cold treatment at 3°C for 48 h. Gene expression was determined by RT-qPCR using gene-specific primers (Table S2).
(A–E) dehydrins (*MdDHN*) *1, 2, 4, 14, 16*, (F) *MdNAC29a*, (G) *MdNAC104b*, (H) *MdCBF2*. 35S:EIL1 lines: E310ko, E316ko and E317ox (harvest) or E322ox (cold treatment); CTRL (control) lines and ACO1as (ACC oxidase antisense). Log_{10} relative expression values were used for graphing and analysis, based on normalisation against four reference genes. For the expression of *MdDHN4* and *MdDHN16*, the scale was set as log_{10} and rescale margin was set as 80%. Nd: not detected, the expression values were extremely low. Data are presented as mean ± SE (n = 6). Lowercase letters indicate significant differences at the level of $P < 0.05$ among different lines at each stage based on the one-way ANOVA followed by Duncan's test.

Significantly lower expression levels of *MdPG1*, *MdXTH1* and *MdβGAL* were also detected in the co-suppressed lines E310ko and E316ko at harvest, as well as after cold treatment. For the ACO1as line, *MdPG1* expression was down at harvest, *MdXTH1* expression was lower at both samplings, while *MdβGAL* was expressed at control level at both sampling times (Figure 6B–D).

Expression of *MdAFS1* at harvest was significantly lower in the *MdEIL*-co-suppressed lines E310ko, E316ko and also in ACO1as. After 10 weeks of cold treatment, *MdAFS1* expression remained low in lines E310ko and E316ko, while the expression returned to control levels in ACO1as (Figure 6E). For *MdoOMT1*, a similar expression pattern was observed, with lower expression in both *MdEIL*-co-suppressed lines E310ko, E316ko and ACO1as at harvest, but for ACO1as again no downregulation was observed after 10 weeks of cold treatment (Figure 6F).

Expression analysis of key cold regulated-related genes in MdEIL transgenic lines

A major difference in ripening behaviour between the co-suppressed MdEIL lines and ACO1as was that the ACO1as fruit were significantly softer than E310ko and E316ko after cold treatment in both Season 1 and 2 (Figure 3B; Figure S5). ACO1as fruit also showed significantly higher levels of 2MBA, n-propyl acetate and α-farnesene compared with E310ox and E316ox after cold treatment (Figure 5). To investigate the molecular basis for this difference, RT-qPCR was performed on members of the NAC, CBF and dehydrin families. Dehydrins, also known as Group II late embryogenesis abundant (LEA) proteins, are intrinsically disordered proteins, which have high hydrophilicity and protect membranes, proteins and DNA from the effect of abiotic stresses such as cold, drought and salinity (Sun et al., 2021). CBFs are important regulators involved in cold adaptation responses (An et al., 2021), while several NAC TFs such as *MdNAC029* and *MdNAC104* have been implicated in cold response in apple (An, Li, et al., 2018; Medina et al., 2011).

BLASTP searching identified 19 dehydrin genes (*MdDHN1–19*, Figure S7) and six CBF genes (*MdCBF1–6*, Figure S8) in the apple genome. RT-qPCR screening was initially performed with wild-type 'Royal Gala' fruit to identify which dehydrins, CBFs and NAC TFs were most highly expressed and either induced or repressed after cold treatment for 48 h, either at 0.5°C or 3°C (Figure S9). From these results, *MdDHN1*, *2*, *4*, *14* and *16*, as well as the TFs *MdNAC29*, *MdNAC104* and *MdCBF2* were further characterised in detail (Figure 7).

MdDHN1 showed strong induction in the E317ox line but was not strongly cold-induced (Figure 7A). *MdDH2, 4, 14* and *16* were all cold-induced in the control fruit (Figure 7B–E). *MdNAC29a* showed strong cold induction in the ACO1as line but not in the E310ko, E316ko and E317ox line, while *MdNAC104* was repressed in the control and E317ox line, both at harvest and after 48 h cold treatment (Figure 7F,G). *MdCBF2* was induced by cold in ACO1as line and control line, but not in the MdEIL co-suppressed lines E310ko, E316ko nor in the E317ox line (Figure 7H).

MdEIL transcription factors activate the *MdAFS1*, *MdXTH1* and *MdβGAL* promoters

Expression of *MdAFS1*, *MdoOMT1*, *MdPG1*, *MdXTH1* and *MdβGAL* was downregulated in the MdEIL co-suppressed lines E310ko and E316ko. Therefore, we hypothesised that *MdEIL1–4* TFs promote the expression of *MdAFS1*, *MdoOMT1*, *MdXTH1* and *MdβGAL* either by direct binding and activation, and/or by activating the expression of downstream TFs that bind and activate these promoters. A previous study has demonstrated activation of the *MdPG1* promoter by ethylene and/or *MdEIL1–3* (Tacken et al., 2010). To confirm activation in the other four genes, fragments of the *MdAFS1*, *MdoOMT1*, *MdXTH1* and *MdβGAL* promoters, including the ATG start codon and 5′-UTR, extending 2–3 kb upstream, were cloned from 'Royal Gala' genomic DNA into the pGreenII0800-LUC luciferase reporter vector. *MdoOMT1* in 'Royal Gala' exists as two expressed alleles, *MdoOMT1a* and *MdOMT1b*, and only *MdOMT1b* was cloned successfully (three identical clones), referred to in our study as the *MdoOMT1* promoter.

Dual-luciferase assays indicated that activity of *MdAFS1* promoter was significantly induced by *MdEIL1*, *MdEIL3*, *MdEIL4* and a mixture of *MdEIL1–4* (Figure 8A). *MdEIL3*, *MdEIL4* and a mixture of *MdEIL1–4* showed significant activation of the *MdXTH1* and *MdβGAL* promoters. The *MdoOMT1* promoter showed no activation by any of the MdEIL family members (Figure S10). Our results suggest that *MdEIL3* most strongly activated the three promoters, with 1.82, 1.52 and 2.04 folds of activation on proMdAFS1, proMdXTH1 and proMdβGAL, respectively,

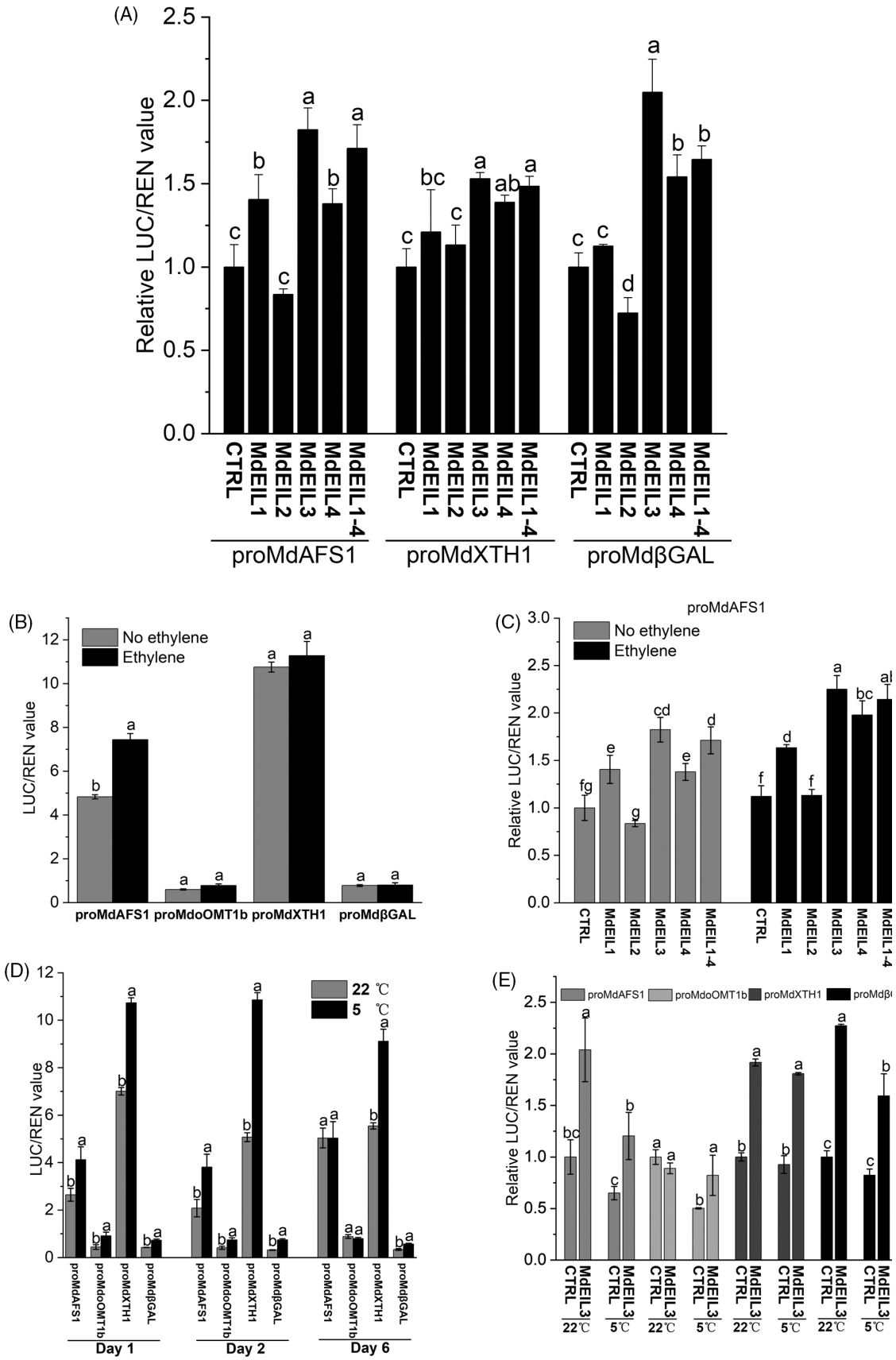

Figure 8. Activation of MdAFS1, MdXTH1 and MdβGAL promoters by MdEIL family members and effects of ethylene and cold treatment on MdAFS1, MdoOMT1, MdXTH1 and MdβGAL promoters alone and MdEIL1–4 or MdEIL3 TFs on the activities of these promoters. Dual-luciferase activity was measured 3 or 4 days after infiltration of *Nicotiana benthamiana* leaves. The LUC/REN value of the empty vector (35S-GUS)/control (CTRL) was set as 1.
(B) Effect of ethylene on the *MdAFS1*, *MdoOMT1*, *MdXTH1* and *MdβGAL* promoters driving the luciferase expression construct.
(C) Effect of ethylene on *MdEIL1–4* overexpression on transcription driven by the *MdAFS1* promoter.
(D) Effect of cold treatment on the *MdAFS1*, *MdoOMT1*, *MdXTH1* and *MdβGAL* promoters driving the luciferase expression construct.
(E) Effect of ethylene on *MdEIL3* overexpression on transcription driven by *MdAFS1* promoter.
For (C) and (E), CTRL: control/empty vector (35S-GUS) without ethylene at 22°C was set as 1, and the value of other treatments were normalised to this value for each promoter separately. Data were presented as mean ± SE (n = 12). Lowercase letters indicate significant differences at the level of $P < 0.05$ among different promoters and stage combinations based on the one-way ANOVA followed by Duncan's test.

followed by *MdEIL4* with 1.37, 1.38 and 1.54 folds of activation respectively, while *MdEIL1* had weaker activation with 1.40, 1.21 and 1.12 folds on the three promoters, respectively, with *MdEIL2* showing no activation on the three promoters tested.

Ethylene and cold treatments enhance effects of MdEIL on promoters

To determine if ethylene had any effect on ripening-related promoter activation or the transactivation of the promoters by MdEIL family members, *Agrobacterium* infiltrated leaves of *N. benthamiana* were treated with ethylene for 24 h (100 ppm) and assessed for luciferase activity according to Tacken et al. (2010). *MdAFS1* promoter activity was significantly upregulated upon ethylene treatment (Figure 8B), but this effect was not observed for the other three promoters tested (*MdoOMT1*, *MdXTH1* and *MdβGAL*). Furthermore, the *MdAFS1* promoter was activated by *MdEIL1*, *MdEIL3*, *MdEIL4* and the mixture of *MdEIL1–4* in the absence of ethylene, but activation was increased when ethylene was supplied (Figure 8C).

To assess if *MdAFS1*, *MdoOMT1*, *MdXTH1* and *MdβGAL* promoters were activated by cold or their transactivation by EIL family members was affected by cold treatment, *N. benthamiana* leaves infiltrated with promoters were treated with cold temperature (5°C) for 24, 48, 144 h and compared to room temperature (22°C), under standard light conditions. Significant upregulation was observed in *MdAFS1*, *MdoOMT1*, *MdXTH1* and *MdβGAL* promoter activation after 24 and 48 h of cold treatment compared to 22°C. However, only the activities of the *MdXTH1* and *MdβGAL* promoters were upregulated by prolonged cold treatment for 144 (Figure 8D), indicating the effect of cold treatment may sometimes act for a short time period in the *N. benthamiana* leaf system. The transactivation by *MdEIL3* on *MdAFS1*, *MdoOMT1*, *MdXTH1* and *MdβGAL* promoters was subsequently assessed after 24 of cold treatment compared with 22°C. No significant upregulation was observed for *MdEIL3* on *MdXTH1* promoter, however, significantly less activation by *MdEIL3* on *MdAFS1* and *MdβGAL* promoters in the cold versus room temperature was observed. For *MdoOMT1* promoter, no activation of *MdEIL3* was found at ambient temperature as observed before, but significant upregulation was observed after 24 h of 5°C cold treatment (Figure 8E).

MdEIL binding to ripening promoters

The A(C/T)G(A/T)A(C/T)CT conserved DNA binding motif has been reported as a conserved EIN3-binding site (Dietzen et al., 2020; Kosugi & Ohashi, 2000). *MdAFS1* and *MdβGAL* promoters were chosen to identify and validate possible EIL binding sites in ripening genes. Both promoters showed one predicted binding motif (Figure 9). To test if these predicted binding motifs were relevant for promoter activation, serial deletions of −1026, −404 and −223 bp upstream of the ATG for the *MdAFS1* promoter and −1068, −1024, −503 and −328 bp for the *MdβGAL* promoter were cloned into the pGreenII0800-LUC reporter vector, respectively (Figure 9A,C). *MdEIL3* was chosen as this TF showed the highest promoter activation with all promoters tested in our study. The −2000 bp, −1026 bp, −404 bp and −223 bp proMdAFS1 fragments were all significantly activated by *MdEIL3*, showing between 1.9- and 2.2-fold activation (Figure 9B), supporting the hypothesis that an EIL binding site might be located in the −89 bp region of the *MdAFS1* promoter, close to the predicted transcription start site (Figure S11). For the *MdβGAL* promoter, there was no significant difference in activation between any of the fragments analysed (Figure 9D), suggesting that either an *MdEIL3* binding is located in the 5′-UTR between −328 bp and the ATG (the predicted 5′-UTR is 676 bp long, Figure S11), or that *MdEIL3* activates another endogenous TF that can bind in this region and activate the *MdβGAL* promoter indirectly.

In vitro binding of *MdEILs* to the proMdAFS1 EIL binding site

Electrophoretic mobility shift assays (EMSAs) were undertaken to directly test for binding of three MdEIL TFs (*MdEIL1–3*) to the EIL binding site in the *MdAFS1* promoter (Figure 9E). The predicted EIL binding domains were overexpressed in *E. coli* as maltose binding protein fusions (MBP) and purified by Ni^{2+} affinity to more than 95% purity as assessed by reducing/denaturing SDS-PAGE (sodium dodecyl sulphate-polyacrylamide gel electrophoresis). The

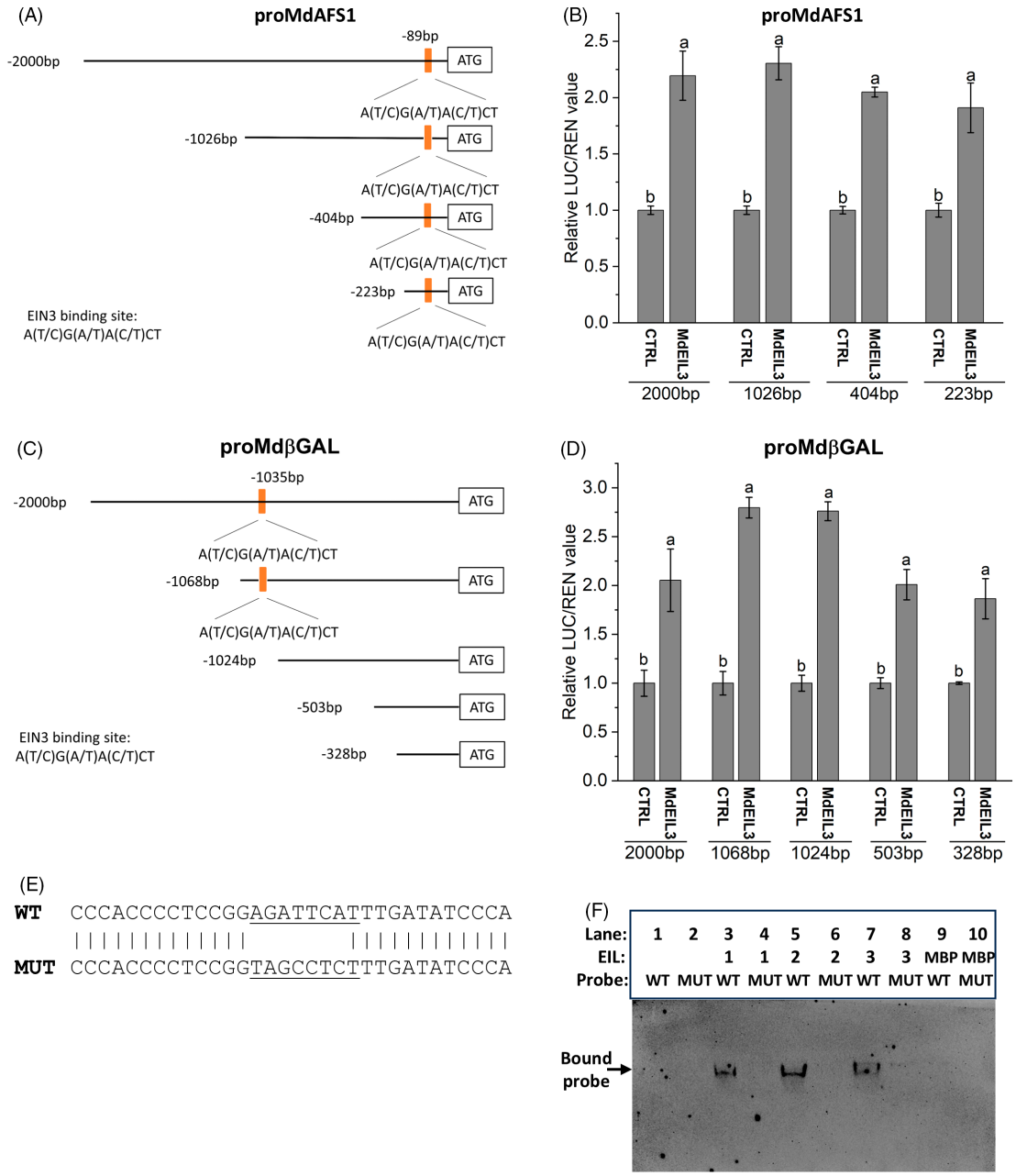

Figure 9. Luciferase reporter activation assays of *MdAFS1* and *MdβGAL* promoters by EIL TF combinations and electrophoretic mobility shift assays (EMSAs) of *MdEIL1, 2, 3* binding to the *MdAFS1* promoter.

(A) Schematic diagram of the *MdAFS1* promoter deleted to −1026 bp, −404 bp and − 223 bp fragments based on the EIL binding site.

(B) Regulatory effects of *MdEIL3* overexpression on transcription driven by the −1026 bp, −404 bp and −223 bp proMdAFS1 fragments.

(C) Schematic diagram of the *MdβGAL* promoter deleted to −1068 bp, −1024 bp and − 503 bp and −328 bp fragments based on the EIL binding site.

(D) Regulatory effects of *MdEIL3* overexpression on transcription driven by the −1068 bp, −1024 bp and −503 bp and −328 bp proMdβGAL fragments. Dual-luciferase activity was measured 3/4 d after infiltration of *N. benthamiana* leaves. The LUC/REN value of empty vector (35S-GUS)/control (CTRL) was set as 1. Data were presented as mean ± SE ($n = 12$). Lowercase letters indicate significant differences at the level of $P < 0.05$ among different combinations based on one-way ANOVA followed by Duncan's test.

(E) Sequence alignment of wild-type (WT) and mutant proMdAFS1 probes used for EMSA with the EIL core underlined. EIL binding motif of WT: AGATTCAT and MUT: TAGCCTCT.

(F) EMSAs of 3′-biotin-labelled proMdAFS1 double-strand DNA probes with *MdEIL1, 2, 3* DNA binding domain proteins. Lane 1, WT DNA probe only, no protein; lane 2, MUT DNA probe only, no protein; lane 3 to 10, WT or MUT probe incubated with MdEIL1, 2, 3 or MBP protein combinations. WT, wild-type; MUT, mutant; MBP, maltose binding protein.

results of EMSA demonstrated that specific binding was observed between a biotin-labelled 32 bp double-strand DNA fragment of the pro*MdAFS1* EIL binding site and MdEIL1, −2 and −3-MBP fusion protein (lane 3, 5, 7), but not to the MBP protein alone (lane 9) (Figure 9F). In contrast, the equivalent 32 bp fragment from the *MdAFS1* promoter with a mutated EIL core-binding motif showed no capacity to bind to the EIL TF proteins (Figure 9F). Together with the transient reporter system, these results demonstrate that the MdEILs interact with the predicted EIL binding site in proMdFAS1, controlling α-farnesene production in apple fruit.

DISCUSSION

EIL genes are important for ethylene-dependent apple fruit ripening

EIN3/EIL TFs are known to act as positive regulators of ethylene responses (Chang et al., 2013), however, a detailed understanding of their contribution to apple fruit ripening has been lacking. To examine the role of MdEILs in apple fruit ripening and in response to cold, we generated transgenic lines to manipulate *MdEIL1* expression. Two transgenic lines E310ko and E316ko showed strong evidence of gene silencing/co-suppression of all four MdEIL genes expressed in ripe fruit (Figure 1), and two transgenic lines (E317ox, E322ox) showed evidence for *MdEIL1* overexpression. Significantly lower expression levels of ethylene-related genes, *ACO1*, cell wall genes, *MdPG1*, *MdXTH1*, *MdβGAL* and volatile biosynthetic genes, *MdAFS1*, *MdoOMT1* were detected in the MdEILko lines at harvest and after cold treatment (Figure 6). As a consequence, fruit from these lines released very little ethylene, were firmer (Figures 3 and 4) and produced lower concentrations of ripe aroma volatiles. One of the MdEILox lines showed opposite effects and was softer than the control and produced more ethylene, both at harvest and after cold treatment.

The reduction in ethylene-dependent fruit ripening processes in the MdEILko lines was similar to that observed in previously characterised transgenic lines in which the ethylene biosynthetic gene ACC oxidase was downregulated by an antisense construct to produce ACOas lines (Johnston et al., 2009; Schaffer et al., 2007). However, the effects of MdEIL co-suppression were generally more pronounced with firmer fruit at harvest and lower levels of aroma volatiles such as α-farnesene, estragole and several fruit esters such as 2-MBA and butyl butanoate being produced. The skin colour development was also affected in both ACOas and MdEILko lines, which fits the model that *MdEIL1* signalling promotes MdMYB1 promoter activation and expression, resulting in positive regulation of anthocyanin biosynthesis/red pigmentation in the fruit apple skin (An et al., 2018b). On the other hand, the SSC was not affected in any of the MdEILox, ko or ACO1as lines, indicating SSC levels act relatively independent of ethylene signalling. These results are similar to that observed after treatment of apples with 1-MCP, where SSC was found to be relatively unaffected postharvest with this potent inhibitor of ethylene signalling (Bai et al., 2005; Fan et al., 1999). Together, these results confirm the importance of MdEILs as key regulators of ethylene-dependent ripening processes in apple fruit.

MdEILs act as transcriptional activators by interaction with ripening-related genes

As TFs, the EIN3/EIL gene family can activate or repress the expression of target genes by binding to target promoters and regulating ethylene-related responses (Shi et al., 2012). In kiwifruit, *AdEIL* activated the *AdACO1* and *AdXET5* promoters (Yin et al., 2010), whilst in melon *CmEIL1* and *2* promoted the activity of *CmACO1* (Huang et al., 2010). *MdEIL1* has been shown to bind to the *MdMYB1* promoter to positively regulate anthocyanin biosynthesis and red colouration in apple fruit (An et al., 2018b). *MdEIL1* has also been shown to bind to the *MdERF1B* promoter *in vitro* and *in vivo*, inducing its expression (Wang et al., 2022). In transient assays, MdEIL2 and MdEIL3 TFs activated the *MdPG1* promoter in the presence of ethylene in apple (Tacken et al., 2010).

To further explore the relationship between MdEIL TFs and apple ripening-related gene expression, we selected *MdAFS1*, *MdoOMT1*, *MdXTH1* and *MdβGAL* as potential target genes. Dual-luciferase assays showed that *MdEIL3* showed the strongest activation on *MdAFS1*, *MdXTH1* and *MdβGAL* promoters, followed by *MdEIL4*. *MdEIL1* showed weaker activation and *MdEIL2* showed no activation on the promoters tested (Figure 7). The activity of *MdoOMT1b* promoter showed no activation by any of the MdEIL family members at room temperature (Figure S10), but was activated by *MdEIL3* in the cold. Analysis of *MdAFS1* and *MdβGAL* genes showed predicted EIL binding sites in both promoters. MdEIL3 was shown to activate the *MdAFS1* promoter (Figures 9) and to directly bind to the EIL binding site at −89 bp upstream of the ATG as was shown by EMSA. Thus, for MdAFS1, MdEILs likely act as direct transcriptional activators. Although MdEIL1–3 were shown to activate *MdβGAL* expression, the binding site is yet to be resolved. In this case, and for other ripening-related genes, activation may either occur directly or indirectly in concert with other TFs.

MdEIL genes play a role in cold response-dependent fruit ripening

After cold treatment, ethylene release from many different fruit is reduced, and low temperature has been reported to suppress expression of ethylene biosynthetic genes, especially ACC synthase, resulting in the inhibition of ethylene production (Shi et al., 2012; Yin et al., 2009). In

Arabidopsis, EIN3 predominantly targets ERF1 that is involved in modulating ethylene responses (Dolgikh et al., 2019; Kosugi & Ohashi, 2000), but it also directly binds to the promoters of CBF1–3 to repress their expression (Shi et al., 2012). In ACC oxidase antisense (ACOas) apple fruit suppressed for ethylene production, fruit softening was shown to be induced by cold temperature alone (Tacken et al., 2010). The authors proposed that cold-induced apple fruit softening occurred via upregulation of transcription of *MdPG1* under control of *MdCBF2*.

In this study, we directly compared the cold response of ACOas and MdEILko fruit treated for 10 weeks at 3 or 5°C and then returned to room temperature for 7 days. Ethylene production after cold treatment was strongly suppressed to a similar extent in both ACOas and MdEILko lines. In contrast, MdEILko lines showed reduced cold temperature-induced softening and were firmer than ACOas fruit after treatment (Figure 3B; Figure S5). Volatile production was also more strongly repressed in the MdEILko lines after cold treatment, with E310ox and E316ox showing significantly lower levels of a number of volatiles, including α-farnesene, n-propyl acetate and 2MBA, compared with cold-treated ACO1as (Figure 5). This differential response suggested a new role for MdEIL TFs in apple fruits' response to cold. This was investigated by RT-qPCR analysis in ACOas and MdEILko fruit to test the expression of members in key gene families involved with cold responses, including dehydrins and CBF + NAC TFs. In contrast to the ACO1as line, expression of several cold response-dependent genes (*MdCBF2*, dehydrins *MdDHN2, −14, −16* and *MdNAC29a*) remained cold-repressed in the MdEILko lines. Whether these effects are direct or indirect will be investigated in future studies.

Together, our results confirm that EIL TFs in apple strongly affect ethylene-dependent fruit ripening, but also reveal unexpected effects of EIL TFs on modulating fruit responses to cold temperature treatment.

EXPERIMENTAL PROCEDURES

Phylogenetic analysis and gene cloning

Phylogenetic analysis was conducted with amino acid translations of putative EIL genes from apple and the model plants *A. thaliana* and *S. lycopersicum*. Apple gene sequences were obtained from the GDR database (https://www.rosaceae.org/). Other gene sequences were obtained from NCBI (https://www.ncbi.nlm.nih.gov/). Multiple alignments were generated, and phylogenetic trees constructed with Geneious Prime Build 2021-11-16, using the Geneious Tree Builder tool.

The control construct 35S:GFP was generated by cloning eGFP (S65T) into the pHEX2 vector (Hellens et al., 2005) by Gateway cloning and driven by the CaMV 35S promoter. The full coding sequence of *MdEIL1* was amplified from 'Royal Gala' apple with gene-specific primers (see Table S2) and cloned in frame with the EGFP gene (S65T) into the pHEX2-35S:GW:eGFP vector. First, the eGFP was PCR amplified with primers containing *Cla*I and *Xba*I restriction sites and ligated into pHEX2 behind the Gateway cloning cassette. Secondly the MdEIL1 ORF without stop codon was amplified and cloned using Gateway cloning following manufacturer's instructions (Invitrogen, USA) into pHEX2-GW-eGFP. The resulting 35S:EIL1 construct has the MdEIL1:eGFP transgene driven by the CaMV 35S promoter. Previous work in tomato has shown that a GFP fusion of *SlEIL1* ('*LeEIL1*') is functional and can partially compensate for the Nr mutation (ethylene receptor mutant) in tomato (Chen et al., 2004).

Generation of transgenic apple plants

The 35S:EIL1 construct was transformed into *Agrobacterium tumefaciens* strain LBA4404 by electroporation. Tissue cultured leaves of 'Royal Gala' apple were used for transformation and transformed leaves were placed on medium containing 100 $\mu g \cdot mL^{-1}$ kanamycin sulphate to regenerate transgenic shoots as previously described (Chen et al., 2022; Yao et al., 1995). Transgenic plants were grafted onto 'M9' rootstock and grown in a containment greenhouse alongside wild-type (WT) 'Royal Gala' and *MdACO1*-antisense (ACO1as, plant AO3) 'Royal Gala' lines (Schaffer et al., 2007). Plants were grown under ambient greenhouse conditions (Souleyre et al., 2014) and hand-pollinated with 'Granny Smith' as the pollen donor. 35S:EIL1 and 35S:GFP trees typically carried <25 fruit per tree. Fruit on WT and ACO1as trees were thinned to ~20 fruit per tree.

For the harvest time point, apple fruits of the control and all the different transgenic lines were harvested at ~150 days after anthesis (DAA). At this time point control fruit are fully mature, and ethylene production has just commenced (Souleyre et al., 2014). For cold treatment, apple fruits were placed in a ventilated cold room at 3 or 5°C for 10 weeks. Fruits were sampled after being held for a further 7 days at room temperature.

RT-qPCR analysis

For each transgenic and control line at harvest and after cold treatment, six randomised fruits were sampled (two fruit per replicate, three biological replicates). Representative wedges of cortex including skin were cut from around the equator and combined into one tube and powdered before storage at −80°C. Total RNA was extracted using the Spectrum Plant Total RNA Kit. First-strand cDNA was synthesised with the ThermoFisher SuperScript IV synthesis system. RT-qPCR was performed using a LightCycler 480 (Roche Applied Science) with SYBR Green Master Mix (Roche Applied Science) as described previously (Yauk et al., 2014). The reference genes *MdPDi* (MDP0000233444), *MdH1* (MDP0000223691), *MdUBC* (MDP0000223691) and *MdACT* (MDP0000170174) were chosen as the internal control (Storch et al., 2015) and the relative expression levels were normalised to the geometrical mean values (Vandesompele et al., 2002) of the four reference genes and calculated using ΔΔCt method (Fu et al., 2021). Gene-specific primer sequences for RT-qPCR were shown in Table S2.

Phenotypic analysis of apple fruits

Fruit firmness of the flesh was measured twice at the mid-point for each fruit as described previously (sun and shade side) using a fruit texture analyser (Güss model GS14, South Africa) fitted with a 11.1 mm diameter Effegi penetrometer probe, 8.9 mm depth, 10 mm measurement speed (Burdon et al., 2014). The soluble solids content (SSC) of a drop of juice from each fruit was determined using an Atago digital refractometer (PAL-1 Atago). Internal ethylene concentrations were measured according to Schaffer

et al. (2007). Skin colour was measured at the opposite sites of the apple (sun and shade side) using a CR-400 Colorimeter (Minolta) under daylight settings (D65) while the starch pattern index (SPI) was assessed using the method described in Blanpied and Silsby (1992).

For volatile compound analysis, 0.5 g of frozen and ground fruit tissues from different transgenic lines and WT apple were aliquoted into 20 mL brown headspace vials. NaCl (30% w/w) was added while samples were kept frozen until analysis. Volatile analysis by SPME GC–MS was conducted according to Wang et al. (2023) with minor modifications. Volatiles were collected at 40°C for 10 min with agitation, controlled by a multipurpose sampler injection system (Gerstel Mülheim, Germany). SPME fibres (1 cm) coated with 50/30 μM DVB/CAR/PDMS were used for the volatile collection. Separation was effected using a 30 m × 0.25 mm internal diameter × 0.25 μM film thickness DB-WAX UI (Agilent, Santa Clara, CA) capillary GC column in an Agilent7890 GC coupled to a Leco BT time-of-flight mass spectrometer (Leco Corp., St Josephs, MI). Compounds were semi-quantified using single diagnostic ions (e.g. *m/z* 93 ion for terpenes) and identified by comparison with the National Institute of Standards and Technology (NIST) database and literature values. The sample peak areas were converted into $ng \cdot g^{-1}$ fresh weight (FW) by comparison with the internal standard cyclohexanone (2.025 μg per sample) or hexadecane standard added in each sample. All the samples consisted of at least three replicates.

Dual-luciferase promoter activation assays

Target promoters were cloned into pGreenII0800-LUC vector (Hellens et al., 2005) using the primers listed in Table S2. Constructs were then transformed into *A. tumefaciens* strain GV3101 + pSOUP. The *A. tumefaciens* cells were freshly streaked on a plate and grown overnight, then suspended in infiltration buffer (10 μM acetosyringone, 10 mM $MgCl_2$) to an OD_{600} = 0.5 for 2 h. The *A. tumefaciens* cells mixture of empty vector / TF and promoters in a ratio of 2:1 or 9:1 (v/v) were infiltrated into six *N. benthamiana* leaves from three plants. *N. benthamiana* plants were grown in a greenhouse at 22°C, under 16 h light and 8 h darkness. Luciferase (LUC)/Renilla (REN) luciferase activities were detected after 3 or 4 days of infiltration with a dual-luciferase assay kit (Targeting System, America) on 96-well plates using a Victory M200 machine. The regulatory effects of TF on promoters were calculated as the LUC/REN ratios with 12 replicates used for each analysis.

For ethylene treatment, *N. benthamiana* plants infiltrated with 35S-GUS control/TF and promoters (4:1 ratio TF to promoter) were treated with 100 ppm ($\mu L \cdot L^{-1}$) ethylene after infiltration for 3 days and kept in 20 L containers with air mixing and CO_2 capture using solid lime ($CaOH_2$) for 20 h (Tacken et al., 2010). The 35S-GUS vector was generated by Gateway cloning the pENTR™-GUS into pHEX2 according to manufacturer's instructions (Invitrogen). The Luciferase (LUC)/Renilla (REN) luciferase activities were measured after 24 h. For the cold treatment, after 3 days of infiltration with empty vector/TF and promoters, plants were moved to a growth cabinet at 5°C with 8 h light, 16 h dark. As controls plants were moved to a growth cabinet at 22°C with 8 h light, 16 h dark. The Luciferase (LUC) / Renilla (REN) luciferase activities were detected after 24, 48 and 144 h.

Protein expression and electrophoretic mobility shift assays

For protein expression and purification, the N-terminus of the Arabidopsis *EIN3* coding sequence (amino acids 1–314/base pairs 1–942 bp) containing the DNA binding domain (Qiu et al., 2015) were aligned with MdEIL1, MdEIL2 and MdEIL3. The equivalent N-terminus for each gene was cloned into the pMAL-c6T vector to create a recombinant fusion protein behind the His-maltose binding protein (His-MBP) (Primers shown in Table S2). The constructs were transformed into *Escherichia coli* strain BL21 DE3 Codon$^+$ RIL (Agilent, USA). Recombinant protein production was auto-induced at 37°C for 4 h and then 16°C for 48 h as described in Studier (2005), and purification was conducted as previously described (Zeng et al., 2020). The purity of the recombinant proteins was confirmed by SDS-PAGE and protein concentration was detected with a Nanodrop 2000. Samples were stored in 10% (v/v) glycerol in small aliquots at −80°C until further use.

The oligonucleotide probes containing EIL-specific *cis*-elements and its mutant derived from the *MdAFS1* promoter were synthesised and 3′-end biotin-labelled on the forward strand (Macrogen, Korea). The two complementary oligos were mixed in Platinum Taq PCR buffer (Invitrogen, USA) and denatured at 95°C for 5 min in a heat block and allowed to anneal slowly to room temperature. Electrophoretic mobility shift assays were performed as described in Nieuwenhuizen et al., 2015 with minor modifications. For gel electrophoresis, 4%–20% Mini-PROTEAN® TGX™ Precast Protein Gels (Bio-Rad, USA) were used, pre-equilibrated in 0.5x cold TBE buffer and 9 μg of recombinant protein was combined with 0.9 fmol of probe. After transferring to positively charged nylon membrane, the blots were blocked with casein blocking buffer (1% casein in TBS). The His-MBP protein alone and mutant biotin-labelled probe were used as negative controls, and the probe sequences are listed in Table S2.

Statistical analysis

Data were analysed with SPSS 20.0 software and expressed as mean ± SE (standard error). One-way ANOVA analysis was applied and the differences between samples calculated using post hoc Duncan's test were considered significant at the level of $P < 0.05$. Figures were plotted with Origin Pro 2022.

AUTHOR CONTRIBUTIONS

JF, XC, NN carried out physiological, biochemical and molecular analyses; MW conducted the GC–MS analysis, ST made the transgenic plants; JF, JT, NN, RA designed the research, analysed the data and wrote the paper.

ACKNOWLEDGEMENTS

We thank Kularajathevan Gunaseelan, Monica Dragulescu and her team for plant care; Kularajathevan Gunaseelan for technical advice on fruit physiological measurements, Linchuan Fang for help with preliminary analysis, Geeta Chhiba for media preparation; Plant & Food Research's Science Publishing Office for proofreading; Robert Schaffer and Nigel Gapper for reviewing the manuscript and the China Scholarship Council who supported Jiao Feng with living expenses for overseas study (No. 202106850061). This work was funded through Plant & Food Research's Technology Development program derived in part from its Royalty Investment Programme. Open access publishing facilitated by New Zealand Institute for Plant and Food Research Ltd, as part of the Wiley - New Zealand Institute for Plant and Food Research Ltd agreement via the Council of Australian University Librarians.

CONFLICT OF INTEREST

The authors declare no conflicts of interest.

DATA AVAILABILITY STATEMENT

The data underlying this article are available in the article and in its online supplementary material.

SUPPORTING INFORMATION

Additional Supporting Information may be found in the online version of this article.

Figure S1. MdEIL genes in the apple genome. (a) Nucleotide alignment distance matrix (% identity) for the full open treading frames (ORFs) of *MdEIL1–10* and (b) for the DNA binding region only (1 kb 5′ from the start ATG). >65% identity is highlighted in pink. (c) Alignment of deduced amino acid sequences of *Malus domestica* MdEIL1–10, *Arabidopsis thaliana* AtEIL1–5, and AtEIN3 and *Solanum lycopersicum* SlEIL1–4. The different conserved amino acids are coloured (25% threshold). Gene IDs: MdEIL1: MD15G1441000; MdEIL2: MD07G1053800; MdEIL3: MD08G1245800; MdEIL4: MD02G1266200; MdEIL5: MD07G1053500; MdEIL6: MD02G1266300; MdEIL7: MD11G1022400; MdEIL8: MD03G1020800; MdEIL9: MD01G1025900; MdEIL10: MD15G1327300; AtEIL1: Q9SLH0.1; AtEIL2: O23115.1; AtEIL3: O23116.1; AtEIL4: Q9LX16.1; AtEIL5: Q9FJQ5.1; AtEIN3: O24606.1; SlEIL1: NP_001234541.1; SlEIL2: NP_001234721.1; SlEIL3: NP_001234546.1; SlEIL4: NP_001233931.1. The parameters used for sequence alignment and phylogenetic tree building are shown at the bottom.

Figure S2. Genomic DNA was extracted from the leaves of pHEX2:EIL1 lines (E), and pHEX2:eGFP control lines (G) using a NucleoSpin Plant II DNA mini kit (Macherey-Nagel) following manufacturer's instructions. PCR was used to confirm that each line was transgenic using primers designed to amplify the GFP transgene (upper lanes, each sample in duplicate) and primers designed to span the *MdEIL1*-GFP junction (bottom panel, single sample). Primers are given in Table S2. PCR conditions were 94°C for 2 min, 35 cycles of 94°C for 30 s; 58°C for 30 sec and 72°C for 45 sec. MQ: MilliQ water, no template control.

Figure S3. Expression of *MdEIL5* in fruit of transgenic and control lines at harvest and after 10 weeks of cold treatment. Gene expression was determined by RT-qPCR using gene-specific primers (Table S2). pHEX2:EIL1 lines = E308, E310, E316, E317, E318, E322; control lines = G311, G319; wildtype = WT2, WT5, WT7, and ACO1as. The $\log_{10}$ of relative expression values were used for graphing and analysis. Data are presented as mean ± SE ($n = 6$). Lowercase letters indicate significant differences at the level of $P < 0.05$ among different lines.

Figure S4. Photographs of apple fruits at harvest (150 DAFB) from pHEX2:EIL1 lines = E308, E310ko, E316ko, E317ox, E318, E322ox; control lines = G311, G319; wild-type = WT2, WT5, WT7, and ACO1as. N.B. The fruit of transgenic lines E310ko, E316ko and the *MdACO1*as line are clearly greener than all other lines. For scale - the blue trays holding the fruit are 48 × 31 cm.

Figure S5. Ethylene production, firmness, soluble solids content hue angle and starch pattern index (SPI) at harvest and after cold treatment. For Season 1 (2023 harvest), fruit were harvested at 150 DAA and stored for 10 weeks at 5°C and returned to room temperature for 7 days. (a) ethylene concentration, (c) firmness, (e) soluble solids content (SSC), (g) hue angle measured at harvest and after cold treatment and (i) starch pattern index (SPI) measured at harvest. pHEX2:EIL1 lines = E317ox, E310ko, E316ko, control (CTRL) lines = G311, G319 and ACO1as. For Season 2 (2024 harvest), fruit were harvested at 150 DAA and stored for 10 weeks at 3°C. (b) ethylene concentration, (d) firmness, (f) soluble solids content (SSC), (j) starch pattern index (SPI) measured at harvest and after cold treatment and (h) hue angle after cold treatment. pHEX2:EIL1 lines = E317ox, E310ko, E316ko, control (CTRL) lines = G311, G319 and ACO1as.

Figure S6. Loading plots (left, in blue) and biplots (right, in red) of headspace volatiles produced by transgenic and control lines at harvest (a, b) and after cold treatment (c, d) based on loading 1 and 2 or principal component 1 and 2. Groups: ACO1as; EILko lines = E310ko, E316ko; EILox lines = E317ox, E322ox; control and wild-type (WT) lines = G311, G319, WT2, WT5, WT7. Original data were normalised by $\log_{10}$ transformation and mean centering.

Figure S7. Phylogenetic tree of the apple dehydrin (MdDHN) gene family compared to Arabidopsis (ARATH). The following GenBank/Uniprot identifiers from Arabidopsis were used to identify homologues in apple by BLAST searching of the *Malus* × *domestica* 'Golden Delicious' genome GDDH13 v1-1. Arabidopsis: RD29A_ARATH, RD29B-1 (AAB25482), RD29B-2 (OAO95316), HRD11_ARATH, XERO2_ARATH, DHR18_ARATH, XERO1_ARATH, DHLEA_ARATH, COR47_ARATH, ERD10_ARATH, ERD14_ARATH, At4g38410 (AAO39908). Nineteen apple dehydrin homologues MdDHN1–19 were identified. Their gene model numbers are listed in Table S2. Methods: Alignment: Geneious Muscle, Tree: Geneious Tree Builder, Tree build method: UPGMA, Genetic distance model: Jukes-Cantor. Bootstrap: 1000 replicates, support threshold >70%. MdDHN1–12 numbering is based on Falavigna et al. (2015).

Figure S8. Phylogenetic tree of the apple C-repeat binding factor (MdCBF) gene family compared to Arabidopsis (At). Homologues in apple were obtained by BLAST searching of the *Malus* × *domestica* 'Golden Delicious' genome GDDH13 v1-1 (cutoff $<1E^{-50}$) with AtACBF1 (AT4G25490.1), AtCBF2 (AT4G25470.1), AtCBF3 (AT4G25480.1), AtCBF4 (AT5G51990.1), AtDDF1 (AT1G12610.1), AtDDF2 (AT1G63030.1) and apple MdCBF2 – (AP2D7/GU732431). DDF: Dwarf and Delayed Flowering 1. Gene model numbers for apple CBFs are listed in Table S2. Methods: Alignment: Geneious Muscle, Tree: Geneious Tree Builder, Tree build method: UPGMA, Genetic distance model: Jukes-Cantor. Bootstrap: 1000 replicates, support threshold >70%.

Figure S9. Expression of apple dehydrins (*MdDHN1–19*), CBFs (*MdCBF1–6*) and *MdNAC029*, *MdNAC104*. To identify which genes showed evidence of cold induction and/or repression, two post-harvest treatments were screened using RT-qPCR. Harvest 1 (H1) consisted of wildtype 'Royal Gala' fruit that had been stored at 1°C for 10 weeks and were then left to sit at room temperature for 1 week. The sample was then stored at 0.5°C for 48 h (0.5°C). Harvest 2 (H2) fruit was tree harvested, kept at room temperature and subsequently stored at room temperature (H2) or 3°C for 48 h (3°C). For each of the four samplings, cDNA was prepared from three biological reps independently and subsequently pooled into a single pooled sample (four pools in total). Gene names highlighted with blue arrows were selected for further RT-qPCR experiments. Primer pairs that did not amplify in any samples/genes that were not expressed, were not graphed (*MdDHN3*, *7*, *9–13*, *18*; *MdCBF1*, *3*, *4*). Primers are listed in Table S2.

Figure S10. Regulatory effects of *MdEIL* family members overexpression on transcription driven by the *MdoOMT1* promoter. Dual-luciferase activity was measured 3/4 d after infiltration of *N. benthamiana* leaves. The LUC/REN value of empty vector (pHEX2-GUS)/control (CTRL) was set as 1. Data were normalised with control and presented as mean ± SE ($n = 12$). Lowercase letters indicate significant differences at the level of $P < 0.05$ among different combinations.

Figure S11. Mapping of RNAseq reads to identify 5′-UTR regions in *MdAFS1* and *Md*β*GAL*. (a) MD10G1311000: *MdAFS1*, (b)

MD02G1079200: *MdβGAL*. The selected sequences started just downstream of predicted 'TATA' boxes and ends at 'ATG' start codon. The predicted length of 5′-UTR area for proMdAFS1 and proMdβGAL are 110 bp (a) and 650 bp (b), respectively.

Table S1. Chromosome location of *MdEIL1*–*MdEIL10*.

Table S2. Gene specific primers for RT-qPCR, cloning and EMSA.

Table S3. Headspace volatiles in MdEIL, control and ACOas lines.

REFERENCES

Alexander, L. & **Grierson, D.** (2002) Ethylene biosynthesis and action in tomato: a model for climacteric fruit ripening. *Journal of Experimental Botany*, **53**, 2039–2055. Available from: https://doi.org/10.1093/jxb/erf072

Alonso, J.M., **Stepanova, A.N.**, **Solano, R.**, **Wisman, E.**, **Ferrari, S.**, **Ausubel, F.M.** ***et al.*** (2003) Five components of the ethylene-response pathway identified in a screen for weak ethylene-insensitive mutants in Arabidopsis. *Proceedings of the National Academy of Sciences of the United States of America*, **100**, 2992–2997. Available from: https://doi.org/10.1073/pnas.0438070100

An, J.P., **Li, R.**, **Qu, F.J.**, **You, C.X.**, **Wang, X.F.** & **Hao, Y.J.** (2018) An apple NAC transcription factor negatively regulates cold tolerance via CBF-dependent pathway. *Journal of Plant Physiology*, **221**, 74–80.

An, J.P., **Wang, X.F.**, **Li, Y.Y.**, **Song, L.Q.**, **Zhao, L.L.**, **You, C.X.** ***et al.*** (2018) EIN3-LIKE1, MYB1, and ETHYLENE RESPONSE FACTOR3 act in a regulatory loop that synergistically modulates ethylene biosynthesis and anthocyanin accumulation. *Plant Physiology*, **178**, 808–823. Available from: https://doi.org/10.1104/pp.18.00068

An, J.P., **Wang, X.F.**, **Zhang, X.W.**, **You, C.X.** & **Hao, Y.J.** (2021) Apple B-box protein BBX37 regulates jasmonic acid mediated cold tolerance through the JAZ-BBX37-ICE1-CBF pathway and undergoes MIEL1-mediated ubiquitination and degradation. *New Phytologist*, **229**, 2707–2729. Available from: https://doi.org/10.1111/nph.17050

Artlip, T.S., **Wisniewski, M.E.** & **Norelli, J.L.** (2014) Field evaluation of apple overexpressing a peach CBF gene confirms its effect on cold hardiness, dormancy, and growth. *Environmental and Experimental Botany*, **106**, 79–86. Available from: https://doi.org/10.1016/j.envexpbot.2013.12.008

Atkinson, R.G., **Sutherland, P.W.**, **Johnston, S.L.**, **Gunaseelan, K.**, **Hallett, I.C.**, **Mitra, D.** ***et al.*** (2012) Down-regulation of POLYGALACTURONASE1 alters firmness, tensile strength and water loss in apple (*Malus* x *domestica*) fruit. *BMC Plant Biology*, **12**, 129. Available from: https://doi.org/10.1186/1471-2229-12-129

Bai, J.H., **Baldwin, E.A.**, **Goodner, K.L.**, **Mattheis, J.P.** & **Brecht, J.K.** (2005) Response of four apple cultivars to 1-methylcyclopropene treatment and controlled atmosphere storage. *HortScience*, **40**, 1534–1538. Available from: https://doi.org/10.21273/Hortsci.40.5.1534

Bai, Y. & **Lindhout, P.** (2007) Domestication and breeding of tomatoes: what have we gained and what can we gain in the future? *Annals of Botany*, **100**, 1085–1094. Available from: https://doi.org/10.1093/aob/mcm150

Barrero-Gil, J. & **Salinas, J.** (2017) CBFs at the crossroads of plant hormone signaling in cold stress response. *Molecular Plant*, **10**, 542–544. Available from: https://doi.org/10.1016/j.molp.2017.03.004

Barry, C.S., **Llop-Tous, M.I.** & **Grierson, D.** (2000) The regulation of 1-aminocyclopropane-1-carboxylic acid synthase gene expression during the transition from system-1 to system-2 ethylene synthesis in tomato. *Plant Physiology*, **123**, 979–986. Available from: https://doi.org/10.1104/pp.123.3.979

Blanpied, G.D. & **Silsby, K.** (1992) Predicting harvest date windows for apples. *Information Bulletin*, **221**, 1–12.

Burdon, J., **Wohlers, M.**, **Pidakala, P.**, **Laurie, T.**, **Punter, M.** & **Billing, D.** (2014) The potential for commonly measured at-harvest fruit characteristics to predict chilling susceptibility of 'Hort16A' kiwifruit. *Postharvest Biology and Technology*, **94**, 41–48. Available from: https://doi.org/10.1016/j.postharvbio.2014.03.005

Chang, K.N., **Zhong, S.**, **Weirauch, M.T.**, **Hon, G.**, **Pelizzola, M.**, **Li, H.** ***et al.*** (2013) Temporal transcriptional response to ethylene gas drives growth hormone cross-regulation in Arabidopsis. *eLife*, **2**, e00675. Available from: https://doi.org/10.7554/eLife.00675 ARTN e00675.

Chen, G., **Alexander, L.** & **Grierson, D.** (2004) Constitutive expression of EIL-like transcription factor partially restores ripening in the ethylene-insensitive *Nr* tomato mutant. *Journal of Experimental Botany*, **55**, 1491–1497. Available from: https://doi.org/10.1093/jxb/erh168

Chen, J., **Tomes, S.**, **Gleave, A.P.**, **Hall, W.**, **Luo, Z.**, **Xu, J.** ***et al.*** (2022) Significant improvement of apple (*Malus domestica* Borkh.) transgenic plant production by pre-transformation with a baby boom transcription factor. *Horticulture Research*, **9**, uhab014. Available from: https://doi.org/10.1093/hr/uhab014

Chinnusamy, V., **Ohta, M.**, **Kanrar, S.**, **Lee, B.H.**, **Hong, X.H.**, **Agarwal, M.** ***et al.*** (2003) ICE1: a regulator of cold-induced transcriptome and freezing tolerance in Arabidopsis. *Genes & Development*, **17**, 1043–1054. Available from: https://doi.org/10.1101/gad.1077503

Deng, H., **Chen, Y.**, **Liu, Z.**, **Liu, Z.**, **Shu, P.**, **Wang, R.** ***et al.*** (2022) SlERF.F12 modulates the transition to ripening in tomato fruit by recruiting the co-repressor TOPLESS and histone deacetylases to repress key ripening genes. *The Plant Cell*, **34**, 1250–1272. Available from: https://doi.org/10.1093/plcell/koac025

Dietzen, C., **Koprivova, A.**, **Whitcomb, S.J.**, **Langen, G.**, **Jobe, T.O.**, **Hoefgen, R.** ***et al.*** (2020) The transcription factor EIL1 participates in the regulation of sulfur-deficiency response. *Plant Physiology*, **184**, 2120–2136. Available from: https://doi.org/10.1104/pp.20.01192

Ding, J.P. & **Pickard, B.G.** (1993) Mechanosensory calcium-selective cation channels in epidermal-cells. *The Plant Journal*, **3**, 83–110.

Dolgikh, V.A., **Pukhovaya, E.M.** & **Zemlyanskaya, E.V.** (2019) Shaping ethylene response: the role of EIN3/EIL1 transcription factors. *Frontiers in Plant Science*, **10**, 1030. Available from: https://doi.org/10.3389/fpls.2019.01030

Ebrahimi, A., **Khajavi, M.Z.**, **Ahmadi, S.**, **Mortazavian, A.M.**, **Abdolshahi, A.**, **Rafiee, S.** ***et al.*** (2022) Novel strategies to control ethylene in fruit and vegetables for extending their shelf life: a review. *International Journal of Environmental Science and Technology*, **19**, 4599–4610. Available from: https://doi.org/10.1007/s13762-021-03485-x

Falavigna, V.D., **Miotto, Y.E.**, **Porto, D.D.**, **Anzanello, R.**, **dos Santos, H.P.**, **Fialho, F.B.** ***et al.*** (2015) Functional diversification of the dehydrin gene family in apple and its contribution to cold acclimation during dormancy. *Physiologia Plantarum*, **155**, 315–329. Available from: https://doi.org/10.1111/ppl.12338

Fan, X.T., **Blankenship, S.M.** & **Mattheis, J.P.** (1999) 1-Methylcyclopropene inhibits apple ripening. *Journal of the American Society for Horticultural Science*, **124**, 690–695. Available from: https://doi.org/10.21273/Jashs.124.6.690

Fenn, M.A. & **Giovannoni, J.J.** (2021) Phytohormones in fruit development and maturation. *The Plant Journal*, **105**, 446–458. Available from: https://doi.org/10.1111/tpj.15112

Fu, B.-I., **Wang, W.**, **Liu, X.**, **Duan, X.**, **Allan, A.C.**, **Grierson, D.** ***et al.*** (2021) An ethylene-hypersensitive methionine sulfoxide reductase regulated by NAC transcription factors increases methionine pool size and ethylene production during kiwifruit ripening. *New Phytologist*, **232**, 237–251. Available from: https://doi.org/10.1111/nph.17560

Gagne, J.M., **Smalle, J.**, **Gingerich, D.J.**, **Walker, J.M.**, **Yoo, S.D.**, **Yanagisawa, S.** ***et al.*** (2004) EIN3-binding F-box 1 and 2 form ubiquitin-protein ligases that repress ethylene action and promote growth by directing EIN3 degradation. *Proceedings of the National Academy of Sciences of the United States of America*, **101**, 6803–6808. Available from: https://doi.org/10.1073/pnas.0401698101

Giovannoni, J., **Nguyen, C.**, **Ampofo, B.**, **Zhong, S.L.** & **Fei, Z.J.** (2017) The epigenome and transcriptional dynamics of fruit ripening. *Annual Review of Plant Biology*, **68**, 61–84. Available from: https://doi.org/10.1146/annurev-arplant-042916-040906

Gunaseelan, K., **McAtee, P.A.**, **Nardozza, S.**, **Pidakala, P.**, **Wang, R.**, **David, K.** ***et al.*** (2019) Copy number variants in kiwifruit ETHYLENE RESPONSE FACTOR/APETALA2 (ERF/AP2)-like genes show divergence in fruit ripening associated cold and ethylene responses in C-REPEAT/DRE BINDING FACTOR-like genes. *PLoS One*, **14**, e0216120. Available from: https://doi.org/10.1371/journal.pone.0216120

Guo, H. & **Ecker, J.R.** (2004) The ethylene signaling pathway: new insights. *Current Opinion in Plant Biology*, **7**, 40–49. Available from: https://doi.org/10.1016/j.pbi.2003.11.011

Hellens, R.P., **Allan, A.C.**, **Friel, E.N.**, **Bolitho, K.**, **Grafton, K.**, **Templeton, M.D.** ***et al.*** (2005) Transient expression vectors for functional genomics, quantification of promoter activity and RNA silencing in plants. *Plant Methods*, **1**, 13. Available from: https://doi.org/10.1186/1746-4811-1-13

Hu, D.-G., **Yu, J.-Q.**, **Han, P.-L.**, **Xie, X.-B.**, **Sun, C.-H.**, **Zhang, Q.-Y.** ***et al.*** (2019) The regulatory module MdPUB29-MdbHLH3 connects ethylene biosynthesis with fruit quality in apple. *New Phytologist*, **221**, 1966–1982. Available from: https://doi.org/10.1111/nph.15511

Huang, S., **Sawaki, T.**, **Takahashi, A.**, **Mizuno, S.**, **Takezawa, K.**, **Matsumura, A.** ***et al.*** (2010) Melon EIN3-like transcription factors (CmEIL1 and CmEIL2) are positive regulators of an ethylene- and ripening-induced 1-aminocyclopropane-1-carboxylic acid oxidase gene (CM-ACO1). *Plant Science*, **178**, 251–257. Available from: https://doi.org/10.1016/j.plantsci.2010.01.005

Huang, W., **Hu, N.**, **Xiao, Z.**, **Qiu, Y.**, **Yang, Y.**, **Yang, J.** ***et al.*** (2022) A molecular framework of ethylene-mediated fruit growth and ripening processes in tomato. *The Plant Cell*, **34**, 3280–3300. Available from: https://doi.org/10.1093/plcell/koac146

Jeong, H.-J., **Choi, J.Y.**, **Shin, H.Y.**, **Bae, J.-M.** & **Shin, J.S.** (2014) Seed-specific expression of seven Arabidopsis promoters. *Gene*, **553**, 17–23. Available from: https://doi.org/10.1016/j.gene.2014.09.051

Ji, Y. & **Wang, A.** (2021) Recent advances in phytohormone regulation of apple-fruit ripening. *Plants (Basel)*, **10**(10), 2061. Available from: https://doi.org/10.3390/plants10102061

Johnston, J.W., **Gunaseelan, K.**, **Pidakala, P.**, **Wang, M.** & **Schaffer, R.J.** (2009) Co-ordination of early and late ripening events in apples is regulated through differential sensitivities to ethylene. *Journal of Experimental Botany*, **60**, 2689–2699. Available from: https://doi.org/10.1093/jxb/erp122

Juurakko, C.L., **diCenzo, G.C.** & **Walker, V.K.** (2021) Cold acclimation and prospects for cold-resilient crops. *Plant Stress*, **2**, 100028. Available from: https://doi.org/10.1016/j.stress.2021.100028

Khan, M.A., **Olsen, K.M.**, **Sovero, V.**, **Kushad, M.M.** & **Korban, S.S.** (2014) Fruit quality traits have played critical roles in domestication of the apple. *The Plant Genome*, **7**, 1–18. Available from: https://doi.org/10.3835/plantgenome2014.04.0018

Kosugi, S. & **Ohashi, Y.** (2000) Cloning and DNA-binding properties of a tobacco ethylene-Insensitive3 (EIN3) homolog. *Nucleic Acids Research*, **28**, 960–967. Available from: https://doi.org/10.1093/nar/28.4.960

Kou, X.H., **Feng, Y.**, **Yuan, S.**, **Zhao, X.Y.**, **Wu, C.**, **Wang, C.** ***et al.*** (2021) Different regulatory mechanisms of plant hormones in the ripening of climacteric and non-climacteric fruits: a review. *Plant Molecular Biology*, **107**, 477–497. Available from: https://doi.org/10.1007/s11103-021-01199-9

Li, S., **Chen, K.S.** & **Grierson, D.** (2021) Molecular and hormonal mechanisms regulating fleshy fruit ripening. *Cells*, **10**(5), 1136. Available from: https://doi.org/10.3390/cells10051136

Li, T., **Jiang, Z.**, **Zhang, L.**, **Tan, D.**, **Wei, Y.**, **Yuan, H.** ***et al.*** (2016) Apple (Malus domestica) MdERF2 negatively affects ethylene biosynthesis during fruit ripening by suppressing MdACS1 transcription. *The Plant Journal*, **88**, 735–748. Available from: https://doi.org/10.1111/tpj.13289

Lin, Z., **Zhong, S.** & **Grierson, D.** (2009) Recent advances in ethylene research. *Journal of Experimental Botany*, **60**, 3311–3336. Available from: https://doi.org/10.1093/jxb/erp204

Liu, M.Y., **Wang, C.R.**, **Ji, H.L.**, **Sun, M.X.**, **Liu, T.Y.**, **Wang, J.H.** ***et al.*** (2024) Ethylene biosynthesis and signal transduction during ripening and softening in non-climacteric fruits: an overview. *Frontiers in Plant Science*, **15**, 1368692. Available from: https://doi.org/10.3389/fpls.2024.1368692

Los, K.K.D., **Schemberger, M.O.**, **Stroka, M.A.**, **Pinto, C.A.**, **Galvao, C.W.**, **Etto, R.M.** ***et al.*** (2024) Relative expression of genes related to volatile organic compounds in non-climacteric and climacteric melons. *Acta Scientiarum Agronomy*, **46**(1), e66350. Available from: https://doi.org/10.4025/actasciagron.v46i1.66350

Ma, Y., **Dai, X.Y.**, **Xu, Y.Y.**, **Luo, W.**, **Zheng, X.M.**, **Zeng, D.L.** ***et al.*** (2015) COLD1 confers chilling tolerance in rice. *Cell*, **160**, 1209–1221. Available from: https://doi.org/10.1016/j.cell.2015.01.046

Martínez-Romero, D., **Bailén, G.**, **Serrano, M.**, **Guillén, F.**, **Valverde, J.M.**, **Zapata, P.** ***et al.*** (2007) Tools to maintain postharvest fruit and vegetable quality through the inhibition of ethylene action:: a review. *Critical Reviews in Food Science and Nutrition*, **47**, 543–560. Available from: https://doi.org/10.1080/10408390600846390

Maruyama-Nakashita, A., **Nakamura, Y.**, **Tohge, T.**, **Saito, K.** & **Takahashi, H.** (2006) Arabidopsis SLIM1 is a central transcriptional regulator of plant sulfur response and metabolism. *The Plant Cell*, **18**, 3235–3251.

Medina, J., **Catalá, R.** & **Salinas, J.** (2011) The CBFs: three Arabidopsis transcription factors to cold acclimate. *Plant Science*, **180**, 3–11.

Mei, C., **Yang, J.**, **Mei, Q.**, **Jia, D.**, **Yan, P.**, **Feng, B.** ***et al.*** (2023) MdNAC104 positively regulates apple cold tolerance via CBF-dependent and CBF-independent pathways. *Plant Biotechnology Journal*, **21**, 2057–2073.

Nieuwenhuizen, N.J., **Chen, X.**, **Wang, M.Y.**, **Matich, A.J.**, **Perez, R.L.**, **Allan, A.C.** ***et al.*** (2015) Natural variation in monoterpene synthesis in kiwifruit: transcriptional regulation of terpene synthases by NAC and ETHYLENE-INSENSITIVE3-like transcription factors. *Plant Physiology*, **167**, 1243–1258. Available from: https://doi.org/10.1104/pp.114.254367

Payasi, A. & **Sanwal, G.G.** (2010) Ripening of climacteric fruits and their control. *Journal of Food Biochemistry*, **34**, 679–710. Available from: https://doi.org/10.1111/j.1745-4514.2009.00307.x

Pechous, S.W. & **Whitaker, B.D.** (2004) Cloning and functional expression of an (*E*, *E*)-α-farnesene synthase cDNA from peel tissue of apple fruit. *Planta*, **219**, 84–94. Available from: https://doi.org/10.1007/s00425-003-1191-4

Peng, P.H., **Lin, C.H.**, **Tsai, H.W.** & **Lin, T.Y.** (2014) Cold response in *Phalaenopsis aphrodite* and characterization of *PaCBF1* and *PaICE1*. *Plant and Cell Physiology*, **55**, 1623–1635. Available from: https://doi.org/10.1093/pcp/pcu093

Qiu, K., **Li, Z.**, **Yang, Z.**, **Chen, J.**, **Wu, S.**, **Zhu, X.** ***et al.*** (2015) EIN3 and ORE1 accelerate degreening during ethylene-mediated leaf senescence by directly activating chlorophyll catabolic genes in Arabidopsis. *PLoS Genetics*, **11**, e1005399. Available from: https://doi.org/10.1371/journal.pgen.1005399

Rao, M.J., **Zuo, H.** & **Xu, Q.** (2021) Genomic insights into citrus domestication and its important agronomic traits. *Plant Communications*, **2**, 100138. Available from: https://doi.org/10.1016/j.xplc.2020.100138

Schaffer, R.J., **Friel, E.N.**, **Souleyre, E.J.F.**, **Bolitho, K.**, **Thodey, K.**, **Ledger, S.** ***et al.*** (2007) A genomics approach reveals that aroma production in apple is controlled by ethylene predominantly at the final step in each biosynthetic pathway. *Plant Physiology*, **144**, 1899–1912. Available from: https://doi.org/10.1104/pp.106.093765

Shi, Y., **Tian, S.**, **Hou, L.**, **Huang, X.**, **Zhang, X.**, **Guo, H.** ***et al.*** (2012) Ethylene signaling negatively regulates freezing tolerance by repressing expression of CBF and type-a ARR genes in Arabidopsis. *The Plant Cell*, **24**, 2578–2595. Available from: https://doi.org/10.1105/tpc.112.098640

Souleyre, E.J.F., **Bowen, J.K.**, **Matich, A.J.**, **Tomes, S.**, **Chen, X.**, **Hunt, M.B.** ***et al.*** (2019) Genetic control of α-farnesene production in apple fruit and its role in fungal pathogenesis. *The Plant Journal*, **100**, 1148–1162. Available from: https://doi.org/10.1111/tpj.14504

Souleyre, E.J.F., **Chagné, D.**, **Chen, X.**, **Tomes, S.**, **Turner, R.M.**, **Wang, M.Y.** ***et al.*** (2014) The AAT1 locus is critical for the biosynthesis of esters contributing to 'ripe apple' flavour in 'Royal Gala' and 'granny smith' apples. *The Plant Journal*, **78**, 903–915. Available from: https://doi.org/10.1111/tpj.12518

Storch, T.T., **Pegoraro, C.**, **Finatto, T.**, **Quecini, V.**, **Rombaldi, C.V.** & **Girardi, C.L.** (2015) Identification of a novel reference gene for apple transcriptional profiling under postharvest conditions. *PLoS One*, **10**, e0120599. Available from: https://doi.org/10.1371/journal.pone.0120599

Studier, F.W. (2005) Protein production by auto-induction in high-density shaking cultures. *Protein Expression and Purification*, **41**, 207–234. Available from: https://doi.org/10.1016/j.pep.2005.01.016

Sun, Z., **Li, S.**, **Chen, W.**, **Zhang, J.**, **Zhang, L.**, **Sun, W.** ***et al.*** (2021) Plant dehydrins: expression, regulatory networks, and protective roles in plants challenged by abiotic stress. *International Journal of Molecular Sciences*, **22**(23), 12619. Available from: https://doi.org/10.3390/ijms222312619

Tacken, E., **Ireland, H.**, **Gunaseelan, K.**, **Karunairetnam, S.**, **Wang, D.**, **Schultz, K.** ***et al.*** (2010) The role of ethylene and cold temperature in the regulation of the apple *POLYGALACTURONASE1* gene and fruit softening. *Plant Physiology*, **153**, 294–305. Available from: https://doi.org/10.1104/pp.109.151092

Tieman, D.M., **Ciardi, J.A.**, **Taylor, M.G.** & **Klee, H.J.** (2001) Members of the tomato LeEIL (EIN3-like) gene family are functionally redundant and regulate ethylene responses throughout plant development. *The Plant Journal*, **26**, 47–58. Available from: https://doi.org/10.1046/j.1365-313x.2001.01006.x

Vandesompele, J., **De Preter, K.**, **Pattyn, F.**, **Poppe, B.**, **Van Roy, N.**, **De Paepe, A.** ***et al.*** (2002) Accurate normalization of real-time quantitative

RT-PCR data by geometric averaging of multiple internal control genes. *Genome Biology*, **3**, RESEARCH0034.

Vazquez-Hernandez, M., **Romero, I.**, **Escribano, M.I.**, **Merodio, C.** & **Sanchez-Ballesta, M.T.** (2017) Deciphering the role of CBF/DREB transcription factors and dehydrins in maintaining the quality of table grapes cv. Autumn royal treated with high CO_2 levels and stored at 0°C. *Frontiers in Plant Science*, **8**, 1591. Available from: https://doi.org/10.3389/fpls.2017.01591

Velasco, R., **Zharkikh, A.**, **Affourtit, J.**, **Dhingra, A.**, **Cestaro, A.**, **Kalyanaraman, A.** ***et al.*** (2010) The genome of the domesticated apple (*Malus* × *domestica* Borkh.). *Nature Genetics*, **42**, 833–839. Available from: https://doi.org/10.1038/ng.654

Wang, S., **Li, L.-X.**, **Fang, Y.**, **Li, D.**, **Mao, Z.**, **Zhu, Z.** ***et al.*** (2022) MdERF1B–MdMYC2 module integrates ethylene and jasmonic acid to regulate the biosynthesis of anthocyanin in apple. *Horticulture Research*, **9**, uhac142. Available from: https://doi.org/10.1093/hr/uhac142

Wang, W., **Wang, J.**, **Wu, Y.-Y.**, **Li, D.**, **Allan, A.C.** & **Yin, X.** (2020) Genome-wide analysis of coding and non-coding RNA reveals a conserved miR164-NAC regulatory pathway for fruit ripening. *New Phytologist*, **225**, 1618–1634. Available from: https://doi.org/10.1111/nph.16233

Wang, W., **Wang, M.Y.**, **Zeng, Y.**, **Chen, X.**, **Wang, X.**, **Barrington, A.M.** ***et al.*** (2023) The terpene synthase (TPS) gene family in kiwifruit shows high functional redundancy and a subset of TPS likely fulfil overlapping functions in fruit flavour, floral bouquet and defence. *Molecular Horticulture*, **3**(9). Available from: https://doi.org/10.1186/s43897-023-00057-0

Wang, Y. & **Hua, J.** (2009) A moderate decrease in temperature induces COR15a expression through the CBF signaling cascade and enhances freezing tolerance. *The Plant Journal*, **60**, 340–349. Available from: https://doi.org/10.1111/j.1365-313X.2009.03959.x

Weiss, J. & **Egea-Cortines, M.** (2009) Transcriptomic analysis of cold response in tomato fruits identifies dehydrin as a marker of cold stress. *Journal of Applied Genetics*, **50**, 311–319. Available from: https://doi.org/10.1007/Bf03195689

Wi, S.D., **Lee, E.S.**, **Park, J.H.**, **Chae, H.B.**, **Paeng, S.K.**, **Bae, S.B.** ***et al.*** (2022) Redox-mediated structural and functional switching of C-repeat binding factors enhances plant cold tolerance. *New Phytologist*, **233**, 1067–1073. Available from: https://doi.org/10.1111/nph.17745

Xie, Y., **Chen, P.**, **Yan, Y.**, **Bao, C.**, **Li, X.**, **Wang, L.** ***et al.*** (2018) An atypical R2R3 MYB transcription factor increases cold hardiness by CBF-dependent and CBF-independent pathways in apple. *New Phytologist*, **218**, 201–218. Available from: https://doi.org/10.1111/nph.14952

Yang, H., **Liu, J.**, **Dang, M.**, **Zhang, B.**, **Li, H.**, **Meng, R.** ***et al.*** (2018) Analysis of β-galactosidase during fruit development and ripening in two different texture types of apple cultivars. *Frontiers in Plant Science*, **9**, 539. Available from: https://doi.org/10.3389/fpls.2018.00539

Yao, J.-L., **Cohen, D.**, **Atkinson, R.**, **Richardson, K.** & **Morris, B.** (1995) Regeneration of transgenic plants from the commercial apple cultivar Royal Gala. *Plant Cell Reports*, **14**, 407–412. Available from: https://doi.org/10.1007/BF00234044

Yauk, Y.-K., **Chagné, D.**, **Tomes, S.**, **Matich, A.J.**, **Wang, M.Y.**, **Chen, X.** ***et al.*** (2015) The O-methyltransferase gene MdoOMT1 is required for biosynthesis of methylated phenylpropenes in ripe apple fruit. *The Plant Journal*, **82**, 937–950. Available from: https://doi.org/10.1111/tpj.12861

Yauk, Y.-K., **Ged, C.**, **Wang, M.Y.**, **Matich, A.J.**, **Tessarotto, L.**, **Cooney, J.M.** ***et al.*** (2014) Manipulation of flavour and aroma compound sequestration and release using a glycosyltransferase with specificity for terpene alcohols. *The Plant Journal*, **80**, 317–330. Available from: https://doi.org/10.1111/tpj.12634

Yin, X., **Allan, A.C.**, **Chen, K.** & **Ferguson, I.B.** (2010) Kiwifruit EIL and ERF genes involved in regulating fruit ripening. *Plant Physiology*, **153**, 1280–1292. Available from: https://doi.org/10.1104/pp.110.157081

Yin, X., **Allan, A.C.**, **Zhang, B.**, **Wu, R.**, **Burdon, J.**, **Wang, P.** ***et al.*** (2009) Ethylene-related genes show a differential response to low temperature during 'Hayward' kiwifruit ripening. *Postharvest Biology and Technology*, **52**, 9–15. Available from: https://doi.org/10.1016/j.postharvbio.2008.09.016

Yue, P., **Lu, Q.**, **Liu, Z.**, **Lv, T.**, **Li, X.**, **Bu, H.** ***et al.*** (2020) Auxin-activated MdARF5 induces the expression of ethylene biosynthetic genes to initiate apple fruit ripening. *New Phytologist*, **226**, 1781–1795. Available from: https://doi.org/10.1111/nph.16500

Zeng, Y., **Wang, M.Y.**, **Hunter, D.C.**, **Matich, A.J.**, **McAtee, P.A.**, **Knäbel, M.** ***et al.*** (2020) Sensory-directed genetic and biochemical characterization of volatile terpene production in kiwifruit. *Plant Physiology*, **183**, 51–66. Available from: https://doi.org/10.1104/pp.20.00186

Zhang, J.H., **Cheng, D.**, **Wang, B.B.**, **Khan, I.** & **Ni, Y.H.** (2017) Ethylene control technologies in extending postharvest shelf life of climacteric fruit. *Journal of Agricultural and Food Chemistry*, **65**, 7308–7319. Available from: https://doi.org/10.1021/acs.jafc.7b02616

Zhang, Z., **Wang, N.**, **Jiang, S.**, **Xu, H.**, **Wang, Y.**, **Wang, C.** ***et al.*** (2017) Analysis of the xyloglucan endotransglucosylase/hydrolase gene family during apple fruit ripening and softening. *Journal of Agricultural and Food Chemistry*, **65**, 429–434. Available from: https://doi.org/10.1021/acs.jafc.6b04536